Journal Pre-proof

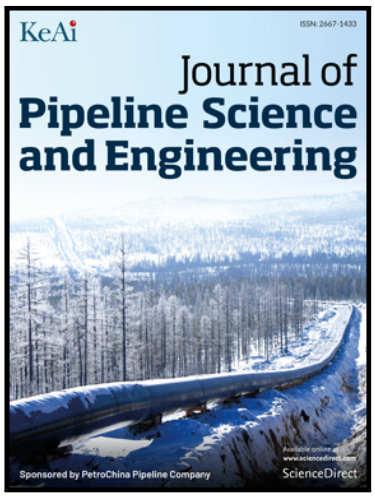

A Comprehensive Review of Polyethylene Pipes: Failure Mechanisms, Performance Models, Inspection Methods, and Repair Solutions

Hao Wang , Jay Shah , Said-El Hawwat , Qindan Huang , Alireza Khatami

PII: S2667-1433(24)00002-7
DOI: https://doi.org/10.1016/j.jpse.2024.100174
Reference: JPSE 100174

To appear in: *Journal of Pipeline Science and Engineering*

Received date: 19 October 2023
Revised date: 10 January 2024
Accepted date: 14 January 2024

Please cite this article as: Hao Wang , Jay Shah , Said-El Hawwat , Qindan Huang , Alireza Khatami , A Comprehensive Review of Polyethylene Pipes: Failure Mechanisms, Performance Models, Inspection Methods, and Repair Solutions, *Journal of Pipeline Science and Engineering* (2024), doi: https://doi.org/10.1016/j.jpse.2024.100174

This is a PDF file of an article that has undergone enhancements after acceptance, such as the addition of a cover page and metadata, and formatting for readability, but it is not yet the definitive version of record. This version will undergo additional copyediting, typesetting and review before it is published in its final form, but we are providing this version to give early visibility of the article. Please note that, during the production process, errors may be discovered which could affect the content, and all legal disclaimers that apply to the journal pertain.

© 2024 The Authors. Publishing Services by Elsevier B.V. on behalf of KeAi Communications Co. Ltd.
This is an open access article under the CC BY-NC-ND license (http://creativecommons.org/licenses/by-nc-nd/4.0/)

Highlights

- Polyethylene (PE) pipes account for up to 90-95% of new gas distribution pipelines in Europe and the United States.
- The failure of a PE pipe is a multivariate problem that can occur due to pre-existing defect growth, material aging, or foundation settlement.
- Long-term hydrostatic strength test results are extrapolated to predict the lifetime performance of the pipeline; however, this method does not account for the effects of material aging.
- The use of ultrasonic testing is highly restricted to the welded sections of PE pipes, relative to its versatile usage in inspecting steel pipes.
- PE demonstrates poor adhesion properties due to its low surface energy, making it challenging to develop adhesion-based repair techniques for incipient surface defects.

Journal Pre-proof

Journal Pre-proof

A Comprehensive Review of Polyethylene Pipes: Failure Mechanisms, Performance Models, Inspection Methods, and Repair Solutions

Hao Wang[1], Jay Shah[2,*], Said-El Hawwat[1], Qindan Huang[3], Alireza Khatami[3]

[1]Department of Civil and Environmental Engineering, Rutgers – The State University of New Jersey, Piscataway, NJ 08854
[2]Centre of Advanced Infrastructure and Transportation, Rutgers – The State University of New Jersey, Piscataway, NJ 08854
[3]Department of Civil, Construction, and Environmental Engineering, Marquette University, Milwaukee, WI 53233

[*]**Corresponding Author:** jayk.shah@rutgers.edu

Email address:
Hao Wang: hwang.cee@rutgers.edu
Jay Shah: jayk.shah@rutgers.edu
Said-El Hawwat: sme96@scarletmail.rutgers.edu
Qindan Huang: qindan.huang@marquette.edu
Alireza Khatami: Alireza.khatami@marquette.edu

Journal Pre-proof

Abstract

Polyethylene (PE) pipes are widely used for natural gas distribution due to their good durability and low costs. To ensure the integrity of PE pipelines, it is crucial to develop a comprehensive understanding of pipe failure mechanisms and to recognize the benefits and limitations of different pipeline monitoring strategies. This review provides an overview of different types of pipe failures in the context of their response to operational loads and material degradation. It also covers the details of mechanical tests for predicting the long-term performance of pipes, theoretical models for studying defect growth, examines different defect detection methods, and concludes with an assessment of pipe repair techniques.

The findings highlight the importance of investigating the effects of existing defects on the operational performance of the pipeline. This indirectly emphasizes the need to develop time- and cost-efficient strategies to detect defects in the early stages. There is a clear gap in the inclusion of PE aging effects in the lifetime performance models. In addition, given the large number of inspection techniques, a regulated selection of pipeline inspection methods is highly desired, specific to the defect type. Further research in advancing adhesive-based repair of incipient defects is crucial to prevent catastrophic defect growth.

Keywords: Polyethylene; Natural gas pipeline; Lifetime prediction models; Pipe failure; Slow crack growth; Ductile failure

1. Introduction

PE pipes account for up to 90-95% of new gas distribution pipelines in Europe and United States [1]. PE as a pipe material offers well-recognized advantages such as lightweight, higher flexibility, and resistance of chemical attack compared to steel pipelines. These pipes are further recognized for their ability to create stronger than material joints typically done through butt fusion and electrofusion welding. Considering the use of PE pipes for natural gas transportation to densely populated commercial and residential properties, explosions due to pipeline failure can have serious consequences to human lives and economic loss. Therefore, the concerns associated with pipeline failure are of top priority to address. It is crucial to develop methodologies for quantitative assessment of pipeline integrity with understanding of the material properties of PE and available techniques for testing and monitoring of such pipes.

PE being a semicrystalline polymer is composed of long chain like molecules of various lengths and side branches [2, 3]. The performance matrix of PE pipes is generally determined by material density (base resin), molecular weight (MW) of polymeric chains, and their distribution [4]. Due to polymeric structure, PE demonstrates viscoelastic behavior resulting in complex creep-stress relaxation behavior [5, 6]. Therefore, short term performance tests such as tensile tests are limited in determining long-term performance of PE pipes. PE response to load is time-dependent in nature and thus long-term hydrostatic test are needed to predict the failure mechanism [7].

For pressurized pipe in operating conditions, the long-term creep rupture curve for a PE pipe that represents the relationship between the applied stress and failure time can be used to describe three prominent failure modes: ductile, quasi-brittle, and brittle failure [8]. The development of different failure modes is dependent on morphology of PE polymeric bonds which are sensitive to service loads and material degradation in extreme environments. Ductile failure dominates at high hoop stress level and has shorter failure time, generally a result of plastic deformation before ultimate failure. The creep rupture curve transitions into most common quasi-brittle failure stage through a mechanical knee at a relatively lower hoop stress and longer failure time [9], and is typically represented with slow crack growth (SCG). This quasi-brittle failure is widely accepted as the benchmark to project the long-term service time of PE pipes. However, considering the large-scale chemical aging of PE polymer in extreme environments, brittle failure can occur in a nearly stress-independent manner shown as a transition through chemical knee [10]. To quantify the in-service performance of the pipe, widely accepted lifetime prediction methods such as hydrostatic testing, and extrapolation techniques mentioned in ISO 9080 and ASTM D2837 are typically used. In addition, various fracture mechanics-based investigations have been reported to investigate the crack propagation in PE pipes [11, 12].

Besides material related failures, other common causes for PE pipe failure include poor fusion of PE joints, third-party damage, and foundation settlement [13, 14]. PE joints are usually prepared through butt-fusion or electro-fusion welding techniques [15, 16]. The success of these joints is subjective to the material inherent properties and the ability of manufacturers to follow the fusion protocols. Insufficient fusion time can result in ductile and brittle failures, whereas joint contamination can result in interfacial voids [17]. The challenges of cold fusion, voids, and cracks in PE joints are most inspected with non-destructive methods such as ultrasonic testing [18-20], radiography [21], and infrared thermography methods [22-24]. Third party-damage usually affects the external surface of the pipe causing surface cracks and

Journal Pre-proof

bending of the material. Any surface crack with a depth beyond 10% of material thickness is considered damage [25, 26]. Foundation settlements due to over-urbanization can also induce man-made deflections in pipes resulting in leaks and bursting failure of pipe. Numerical studies have been conducted to study the pipe response to the operational loads during a foundation settlement [27].

It is evident that the complexity of PE pipeline failure can be subjective to material properties, manufacturing and operational conditions, and third-party damage. Therefore, it is imperative to understand different aspects of pipeline failures to develop robust testing and pipeline maintenance strategies. This paper presents an extensive review of failure types, performance prediction models, inspection techniques, and repair methods for PE pipes. After that, the gaps in the existing studies are identified and the recommendations for further research are provided.

2. Failure Types of PE pipes

2.1 Failure due to Load-Induced Stress

The failure mechanisms in PE pipes can be associated with the semi-crystalline characteristic of PE which is the result of tie molecules holding together the amorphous and lamellar crystal regions. These polymeric reinforcements change under varying stress levels and service periods. The relationship between the applied stress and failure time can be used to describe three prominent failure modes of PE pipes: ductile, quasi-brittle, and brittle failure, as shown in Figure 1.

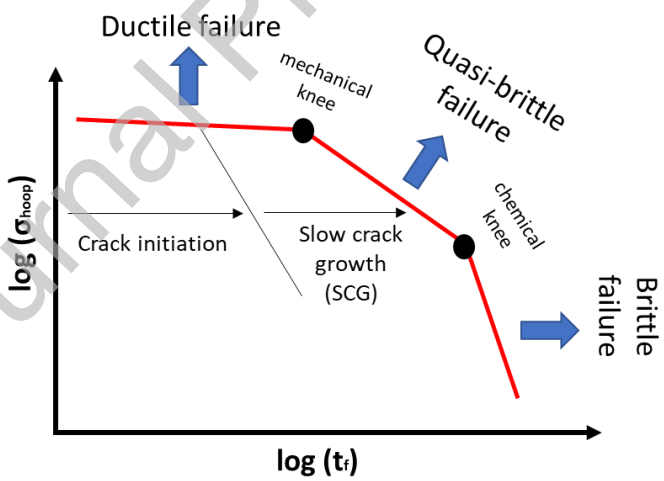

Figure 1. Illustration of relationship between hoop stress and failure time of PE pipes [8]

2.1.1 Ductile Failure

Ductile failure is characterized by material yielding as a response to the stresses in PE pipes, which usually occurs at high-stress levels and indicates shorter failure time. In an ideal scenario, it occurs when the pipe is loaded beyond its yield strength [28, 29]. Over-pressurization causes the pipe diameter to expand, resulting in the pipe wall thinning and stretching to the point where the pipe wall ligament is not capable for resisting the induced large circumferential hoop stresses [30]. Such failure usually shows the signs of necking in a tensile test, bulging from high internal pressure, and collapse when the pipe wall is bent or

Journal Pre-proof

kinking. At the microscopic level, the polymeric chains stretch to their maximum limit resulting in the breakdown of local semi-crystalline structures in high-stress conditions [5, 6].

Ductile failure in PE is typically considered when the creep strain from a constant stress load reaches the critical strain value of 10% as demonstrated in the reported studies [31, 32]. The time for ductile failure (t_D) can be determined experimentally under the assumption of constant stress (σ) and temperature (T) dependence, as shown in Equation (1) [33].

$$t_D = \frac{D \cdot \epsilon_c^{\frac{1}{n}} \cdot \exp(\frac{Q_D}{\mathrm{R}' \cdot T})}{\sigma^{\frac{m}{n}}} \tag{1}$$

Where, ε_c is the critical strain value, m and n are stress dependent material parameters, R′ is gas constant, and D and Q_D are temperature dependent material parameters.

2.1.2 Quasi-Brittle Failure

Quasi-brittle failure, unlike ductile failure, occurs gradually over an extended service period due to the gradual relaxation of polymeric chains. This leads to the formation of a discontinuous crystalline region under low-stress conditions [34, 35]. Experimental observations by Brown et al. [33] have shown that crack initiation in PE pipes leads to a transition from ductile to slow crack growth (SCG), for a specimen is kept at a room temperature of approximately 0.78 times its melting point (~110°C). This transition is a characteristic feature observed in all crystalline materials when subjected to low-stress conditions at high temperatures. Moreover, the non-crystalline region of PE is expected to exhibit rubber-like behavior at testing room temperature, which is typically above the transition temperature for failure mode (i.e., −27ºC). Therefore, a combined effect of high-temperature deflections and rubber-like behavior in the material matrix of PE under low-stress conditions is likely to result in long-term brittle fracture as discussed next.

2.1.3 Brittle Failure

Long-time brittle failure initiates with SCG in the material [36]. Under a constant stress, the failure mode begins with a plastic zone immediately emanating from the stress-concentrated regions at the portions of the SCG with the highest curvature. The initial crack opening displacement (COD) expands at a constant rate depending on stress intensity and material properties without any crack growth. Eventually, when a critical value of COD (δ_c) is reached, crack growth initiates. Beyond this stage, the crack and the plastic zone expand rapidly under operating conditions, until it eventually leads to sudden fracture. The time for brittle failure (t_{bf}) can be determined through notch tests under the assumption of constant stress (σ) and temperature (T) dependence as shown in Equation (2) [33].

$$t_{bf} = \frac{(\alpha a_0 + \delta_c) \cdot \exp(\frac{Q_B}{\mathrm{R}' \cdot T})}{\beta \sigma^p a_0^q} \tag{2}$$

Where, α represents the ratio of COD to the length of the damaged zone, a_0 denotes the depth of the initial notch, and β, p, q, and Q_B are temperature specific material parameters [37, 38].

2.2 Chemical and Thermal Aging

Pipe failure related to thermal aging primarily stems from the degradation properties of PE as a material. The base resin of PE pipe is typically prepared with additives such as antioxidants

Journal Pre-proof

and UV stabilizers to minimize material degradation caused by photo-oxidation and chemical attack [39, 40]. During pipe storage or exposure to the sun, PE can undergo stress-independent chemical or thermal aging, resulting in an irreversible change in its nature. Once the antioxidant layer depletes, the chemical structure of PE changes due to cross-linking and polymeric chain scission, leading to premature polymer degradation. Additionally, exposure of PE to UV radiation results in photodegradation, which, in turn, leads to the formation of free radicals in PE due to the breaking of C-H bonds [41, 42]. These free radicals are highly unstable and result in subsequent polymeric chain scission reactions, occurring long after the UV exposure, eventually leading to brittle failure [43-45].

The concerning aspect of PE pipe aging is its heterogeneous degradation, typically observed as distributed regions of fine cracks. This makes it challenging to assess the actual condition of pipes during pipeline maintenance activities. Figure 2a provides an example where a significant difference between the degradation of the external pipe surface and the internal surface is evident. Additionally, thermally aged pipes exhibit a significant reduction in their load-bearing capacity (Figure 2b), as reported by Chen et al. [46], where the authors aged PE100 pipes under controlled temperature and pressure conditions.

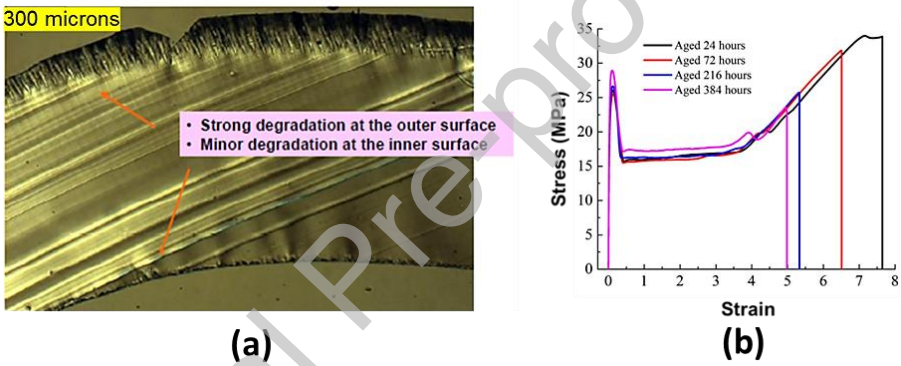

Figure 2. (a) Embrittlement of the external surface of aged PE pipe [40] , and (b) Stress-strain curve for a PE pipe, thermally aged at 95°C under cyclic pressure [46]

2.3 Poorly Fused PE Joints

PE joints are commonly prepared using butt fusion or electrofusion techniques (details in Section 5). In a butt fusion joint, the ends of the pipe section are melted and pushed against each other to allow fusion at a predefined weld pressure, whereas, in electrofusion, pipe sections are melted inside a heating electric collar, and the melted pipe bonds with the collar. Both approaches share some common criteria of surface preparation (including cleaning, cutting, and smoothening) followed by melting the pipe sections. The heating, melting, and cooling cycle is controlled for a specific duration subject to pipe geometry and manufacturer requirements.

The service performance of PE pipe joints depends on environmental and operating conditions in which fusion has been performed [47, 48]. A dusty environment can result in contamination in the fused region causing weak interface. Tayefi et al. [49] demonstrated a shortened fatigue-associated failure time in a contaminated electrofused joint when tested with a servo-hydraulic fatigue machine. Other failure reasons are the poor alignment of the joint sections, over or insufficient heating, interfacial voids, and insufficient welding pressure to

Journal Pre-proof

create the desired weld size. Lu et al. [48] investigated the interplay between the weld pressure and the quality of the butt-welded joints in contaminated conditions. It was established that sufficient weld pressure is desired to achieve relatively better weld quality with a longer lifetime, even in contaminated zones, as determined by a constant tensile test. Insufficient heating can result in the cold fusion of joints that are not strong at the molecular level, even though they pass initial inspection criteria [50]. Shi et al [51] reported the cracking through the wall fitting due to higher stress concentration in the electrofusion coupler near the cold fusion zone whereas Li et al. [52] hypothesized that the existence of voids in the welded region can propagate as cracks inside the material, eventually shortening the service life of pipe. Parmar et al. [53] demonstrated that misaligned pipe sections change the failure mode of the pipe to circumferential cracks compared to axial cracks in aligned pipes.

2.4 Other Failure types

2.4.1 Rapid crack propagation (RCP)

The likelihood of RCP in PE pipes is less than that of SCG, but the consequences can be catastrophic. This type of failure is nicknamed “running failure” because it occurs when a new crack experiences a high growth velocity, reaching 100-300 m/s. The crack usually spread axially for a distance many times the pipe’s diameter [54, 55]. Two conditions need to be met for RCP to occur: (1) the surrounding structure must support the crack driving force without any loss in energy, and (2) the fracture resistance of the material must not increase with increasing crack propagation speed.

2.4.2 Foundation settlement

PE pipes are recognized for their resistance to permanent deformations in operating conditions making them a prime candidate for natural gas transportation in urbanized regions. However, buried gas pipes can experience non-uniform stress distribution in case of foundation settlement resulting in localized stress concentrations, causing pipe deflection, burst, and leakage [27]. Foundation settlement can be a result of poor ground excavation techniques in nearby regions to pipelines, poor soil filling during pipe installation, natural disasters like floods, changes in soil moisture due to over-usage of groundwater in overly populated areas, etc. PE pipe failure due to foundation settlement have been explored in various studies and various aspects of excavation load, and displacement of soil have been explored in context of additional pipeline stresses [14, 56, 57]. A direct influence of foundation settlement on stress levels in PE pipe has been reported by Luo et al. [56] , where the unique aspect is the changing location of maximum Mises stress in the deformed pipe with increasing settlement displacement. In addition, the existence of pre-defects can negatively impact the ultimate load bearing capacity of the pipe in foundation settlement scenario [58].

3. Performance Models of Predicting PE Pipe Failure

3.1 Hydrostatic Pressure Test

The goal of hydrostatic pressure testing is to determine a pipe's hydrostatic strength by filling a pipeline with water to increase its internal pressure beyond its designated capacity while physically monitoring for any potential leakage. This allows the identification of faulty sections

Journal Pre-proof

in the pipeline and is widely used to inspect fused joints. In addition, advanced long-term hydrostatic strength (LTHS) tests are performed at elevated temperatures and pressures to predict the long-term performance of the pipe in service-like conditions, as described in different standards (e.g., ISO 4427-3, EN 1555-3, and EN 12201-3). LTHS results are then extrapolated for up to 50 years (ASTM D1598 - 63T) using the extrapolation method of ISO 9080.

The underlying principle of extrapolation is the rate process method [59, 60], generally described in the form of Arrhenius equation (Equation (3 and 4)) where reaction rate can be represented as a function of temperature as follows,

$$K\ (T) = A\ \cdot \exp\left(-\frac{E}{\mathrm{R}'\cdot T}\right) \tag{3}$$

$$\ln\big(K(T)\big) = C - \frac{E}{\mathrm{R}'T} \tag{4}$$

Here, *K(T)* represents the reaction rate of the process, *T* is the absolute temperature in Kelvins, *E* is activation energy (Joule/mol), R′ is gas constant, and *A* is the frequency factor. Using a similar correlation as in the above equations, a relation between the failure time (t_f) of the pipe, and the hoop stress (σ) and temperature (T) can be defined using Equation (5) for a log-log stress-time profile of LTHS test results,

$$\log\big(t_f\big) = C + \frac{B}{T} + C\log\sigma + \frac{D\log\sigma}{T} \tag{5}$$

where, *A*, *B*, *C*, and *D* are unknown constants that can be determined through multi-regression analysis of experimental data, and these are sensitive to the type of PE material.

3.2 Fracture Mechanics Approach

Recent advancements in PE (e.g., PE 80 and PE 100) are recognized for their resistance towards quasi-brittle failure (resulted from SCG), which is typically related to a pre-existing defect. For a primarily non-defected pipe, LTHS tests can last for up to 13 months [61], and these tests do not provide any quantitative information for SCG which is the most common cause for PE pipe failure. Therefore, fracture mechanics models are implemented to study the quasi-brittle failure mode.

3.2.1 Linear Elastic Fracture Mechanics (LEFM) model

Conventionally developed for metallic pipes, LEFM models has also been implemented on PE material provided the global loading component is within the linear viscoelastic range of the material and the plastic deformation at the crack tip is small [62].

The fracture process in LEFM is characterized based on propagation rate of crack (d*a*/d*t*) depending on stress intensity factor (SIF) K_I, as illustrated in Figure 3 [63]. The process consists of three stages: 1) Stage I: the process starts with an incubation period which is the time to initiation of crack since non-defect status (t_{in}), is identified with a rapid decline in d*a*/d*t* at threshold value K_{Ith}; 2) Stage II: after initiation of crack, it begins to propagate slowly under stress, and this period refers to slow crack growth period (t_{SCG}); 3) Stage III: brittle fracture happens when the SIF exceeds the material fracture toughness, referring to the period from the end of SCG to failure (t_{bf}). Thus, the total failure time (t_f) can be calculated from the summation of three stages, as shown in Equation (6).

$$t_f = t_{in} + t_{SCG} + t_{bf} \tag{6}$$

Journal Pre-proof

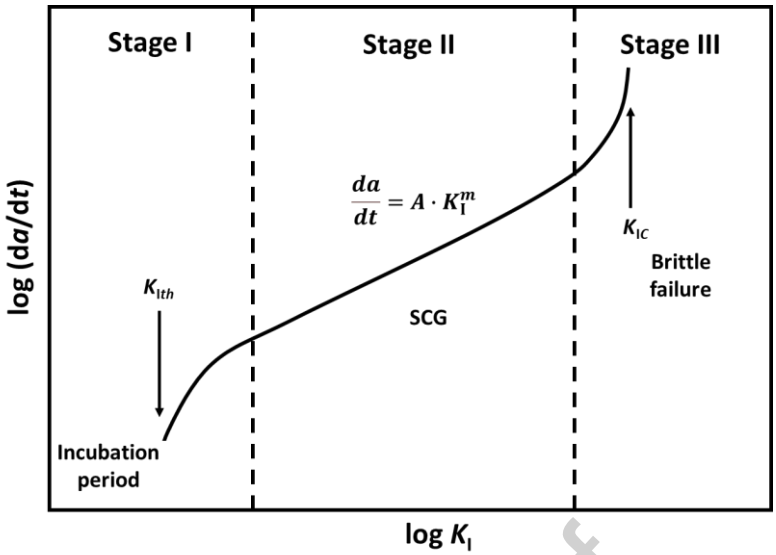

Figure 3. Rate of crack propagation with respect to stress intensity factor [64]

In Stage I (incubation period), the crack can be opened and fully arrested until it reaches a certain threshold of crack opening displacement (COD_{th}). According to ASTM-E1290 test, this threshold can be calculated from Equation (7) [65]. Although the Stage I t_{in} can be a major portion to the pipeline service life, it has been neglected in calculation of the total failure time due to unknown cause of crack formation [63, 66, 67].

$$COD_{th} = \frac{K_I^2(1-\mu^2)}{2\sigma_y E} + \frac{r_p(W-a_0)u_p}{r_p(W-a_0)u_p + a_0 + z} \tag{7}$$

Where, E is the young modulus, σ_y is the yielding stress, μ is Poisson's ratio, r_p is the plastic rotation factor equal to 50.44 and 0.46 for single edge notch bending (SENB) specimens and for compact tension (CT) specimens, respectively, $(W - a_0)$ refers to ligament depth in which w is the width of the test specimen and a_0 is the initial defect depth, u_p is the plastic component of clip gage opening displacement, z is the distance of knife edge measurement point from front face (notched surface) on SENB specimen, or from load line in CT specimen.

In Stage II (i.e., SCG stage), the rate of crack growth can be described based on Paris and Erdogan formula as a function of K_I, as shown in Equation (8) [68].

$$\frac{da}{dt} = A \cdot K_I^m \tag{8}$$

Where, A (mm/s-MPa-m$^{0.5}$) and m (dimensionless) represent the SCG parameters specific to material type, temperature, and loading conditions. This correlation can be used to determine the crack growth kinetics provided the geometric and loading parameters are specified.

In Stage III, the crack growth rate increases sharply as the K_I approaches critical value K_{IC} representing the limit of material fracture toughness. Since the time duration associated with this stage is rather short, it is typically neglected in the calculation of the total failure time. If ignoring the time of crack incubation, Equation (6) is reduced to $t_{bf} \cong t_{SCG}$, which only uses Stage II to conservatively estimate the service life of pipelines subjected to crack growth [63, 66, 67].

In the LEFM model, stress distribution at a crack tip is characterized by stress intensity factor K_I, where "I" specifies the opening mode of crack surface displacement [69, 70], which is the result of in-service loading (e.g., operating pressure, soil loading, residual stress and

Journal Pre-proof

external impact), and current condition of the pipe (e.g., existing surface defects like scratches). Typically, under in-service loadings, a buried plastic pipe is under tensile stress considering only internal pressure on inner and outer surface of the pipe, however, the deflection from soil could exert more tensile stress on the inner surface of the pipe. Therefore, it is commonly assumed that the crack grows from the inner surface of the pipe toward the circumferential direction [71].

Note that K_I is dependent on loading and geometry of the structure and defect. One could extract the value through Finite Element (FE) model. While from a practical point of view, K_I is empirically formulated as a function of applied stress (σ), crack depth (a), and geometric factor Y for most practical applications of pipes as shown in Equation (9) [72, 73].

$$K_I = \sigma \cdot \sqrt{\pi a} \cdot Y \tag{9}$$

For thin-wall pipes, the hoop stress can be calculated as $\sigma = p \cdot r_i / e$ in which p is the internal pressure, r_i is the inner radius of the pipe, and e refers to the wall thickness. Using Equation (9), one can calculate K_I during the crack propagation. In particular, Y is typically formulated as a polynomial function of a/e based on numerical simulations of crack growth considering different geometry of pipes (e.g., [63]).

Therefore, with the calculated values of K_I during the crack propagation, the time for SCG-associated failure, t_f, can be calculated by integrating Equation (8) and imposing limits on crack length from a_i (initial crack depth) to a_f (failure crack depth), as shown in Equation (10). However, it is not easy to determine the failure crack depth, and some studies have set a_f to be the pipe wall thickness.

$$t_{SCG} = \frac{1}{A} \int_{a_i}^{a_f} \frac{1}{K_I^m} da \tag{10}$$

3.2.2 Testing for obtaining LEFM parameters

Simulation of SCG has been conducted using monotonic static loading (e.g., compact tension) on notched pipe ring (NPR) and cracked round bar specimens (CRB) in the literature, respectively [64, 74, 75]. These tests on PE pipe grades typically last for several months, in addition, improvements in the raw materials used in the PE pipes have made it difficult to determine the behavior of SCG using internal pipe pressure tests, especially for modern grades of the classification PE 100 and PE 100-RC. This has resulted in time-consuming and expensive test procedures. To address this, several experimental tests use notched specimen, such as the Notched Pipe Test (NPT) [76], the Pennsylvania Edge-Notch Test (PENT) [77], the Notched Ring Test (NRT) [78] and the Full Notch Creep Test (FNCT) have been developed. To reduce the testing time, temperature was elevated in PENT and NRT [77, 78] and stress cracking liquids were added in FNCT [79].

Recent studies have shown that cyclic round bar (CRB) tests can provide reliable results to calculate mechanical characteristics of SCG within shorter time span [80]. In this approach, specimen is loaded by controlling the loading ratio (R) that is the minimum load to maximum load ratio in one loading cycle; in the elastic range, such ratio is also the minimum stress intensity factor ($K_{I,min}$) to the maximum stress intensity factor ($K_{I,max}$) ratio in one loading cycle. Thus, the change of K_I, ΔK_I ($K_{I,max} - K_{I,min}$), for one loading cycle can be calculated by Equation (11).

$$\Delta K_I = K_{I,max} \cdot (1 - R) \tag{11}$$

Journal Pre-proof

The da/dt can be interpreted based on the growth of crack per number of load cycles (da/dN) and frequency of loading (f) in a cyclic load test through the following equation:

$$\frac{\mathrm{d}a}{\mathrm{d}t} = \frac{\mathrm{d}a}{\mathrm{d}N} \cdot f \tag{12}$$

Through the testing results, (da/dN) and ΔK_{I} are related through Equation (13).

$$\frac{\mathrm{d}a}{\mathrm{d}N} = A \cdot \Delta K_{\mathrm{I}}^{m} \tag{13}$$

Where, A and m are the SCG parameters defined previously in Equation (8), which are unique to the value of R.

A higher value of R means a decrease in the loading range (correspondingly a smaller value of ΔK_{I}) results in a decreasing SCG rate, hence increasing the failure time. Then, the SCG at R = 1 (that corresponds to the static loading) is extrapolated by increasing R in a cyclic testing as shown in Figure 4. Hence, fracture mechanics parameters (A and m at R = 1) can be obtained. Table 1 shows the SCG parameters obtained from the CRB testing for different PE materials at ambient temperature [66, 81].

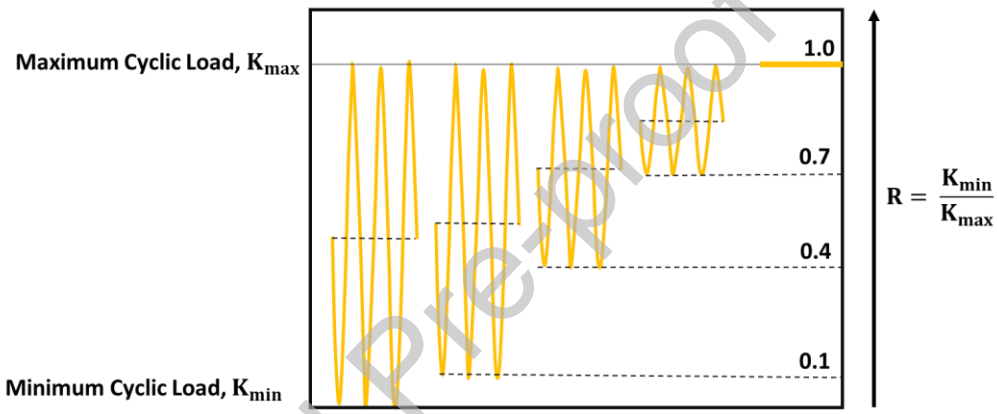

Figure 4. Variation of K_{I} at various R-ratios [82]

Table 1 SCG parameters determined from CRB test at ambient temperature for different PE materials [81]

Material	T(°C)	A	m
PE 80	23	1.83×10^{-6}	7.08
PE 80-MD	23	6.36×10^{-6}	7.79
PE100-RC	23	7.58×10^{-6}	6.73
PE100	23	9.25×10^{-6}	6.28

3.2.3 Elastic plastic fracture mechanics (EPFM) model

Given the constraints of considering only small defects in a LEFM model, the scope of fracture mechanics has been extended to study PE pipes considering extensive deformation and nonlinearity. In general, the ductile fracture is described by four stages in a uniaxial tensile test as shown in Figure 5a based on the crack growth under the loading [71]. The first stage is blunting, where crack is not formed yet, and on the surface, voids can be opened and closed under loading. With the increase in load, blunting affects the molecularizations and crack initiates at the end of opening. With the continuation of the pressure increase, crack starts to develop through the thickness under a stable rate (i.e., SCG) until the unstable tearing occurs.

Journal Pre-proof

The ductile fracture can also be described using four Zones in a burst test based on the relationship between hoop stress and internal pressure of the pipe, as shown in Figure 5b [83]. In particular, Zone I refers to the elastic region, Zone II refers to blunting stage, Zone III refers to the relaxation where the increase in the pressure only increases the volume of the pipe, and the hoop stress remains almost constant, and Zone IV is the hardening. Zone I and Zone II in the burst test are the blunting stage in the uniaxial tensile test in Figure 5a; the end of Zone II and the onset of Zone III correspond to the cracking initiation stage shown in Figure 5a; and Zone III and IV corresponds to the SCG in Figure 5a.

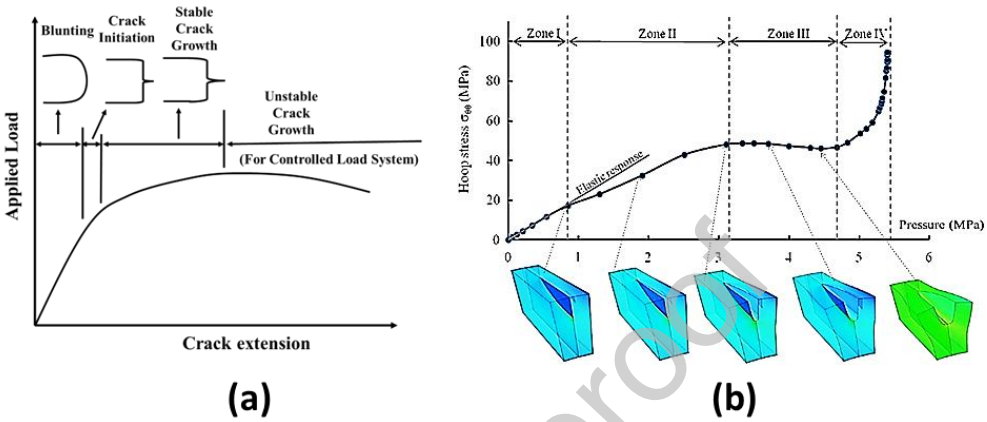

Figure 5. Various stages of crack extension in ductile behavior of plastic observed in (a) Tensile test [71] and (b) Burst test [83]

While LEFM uses SIF to characterize failure at the crack tip, EPFM characterizes the stress distribution based on the released energy per unit area of crack front (kJ/m^2) called "J-integral". Proposed by Rice [84], J-integral based on elastic-plastic fracture mechanics concept provides the estimate to energy available for crack extension in a pre-cracked specimen, which can also be interpreted as crack driving force per unit depth of crack (N/m). Conventionally, J values are determined experimentally using fracture tests that are conducted under a constant displacement rate using specimen configurations such as single edge notched bending (SENB), compact tension (CT) and double edge notched tension (DENT); to follow the crack growth, video-acquisition system or displacement sensors are applied during the loading [85-87]. With the fracture tests, the J value (in either elastic and plastic) can be calculated using Equation (14) considering the elastic and plastic contributions [85, 86, 88].

$$J = J_{\mathrm{el}} + J_{\mathrm{pl}} = \eta_{\mathrm{el}} \frac{U_{\mathrm{el}}}{b \cdot (W-a)} + \eta_{\mathrm{pl}} \frac{U_{\mathrm{pl}}}{b \cdot (W-a)} \tag{14}$$

Where, the subscripts "el" and "pl" refer to elastic and plastic region, η is the geometric factor, U is the energy required for crack expansion, b specimen thickness, and $W - a$ is the ligament length. While U_{el} and U_{pl} can be easily calculated based on the load-displacement curves obtained in the tests, the shape factors (η_{el} and η_{pl}) require a series of tests on various blunt notched specimens with different ligament lengths, specimen geometry, and temperatures.

With the calculated J-value, its relationship with crack growth can be illustrated as a J-a curve (or driving force diagram). As an example, Figure 6 shows the *J-a* curves (in thin solid lines) for a PE pipe under different internal pressures. Alternative to the fracture tests described

Journal Pre-proof

above, *J-a* curves can be obtained using formulas developed by General Electric (GE) Handbook for different ductile materials with different shape and defects [89].

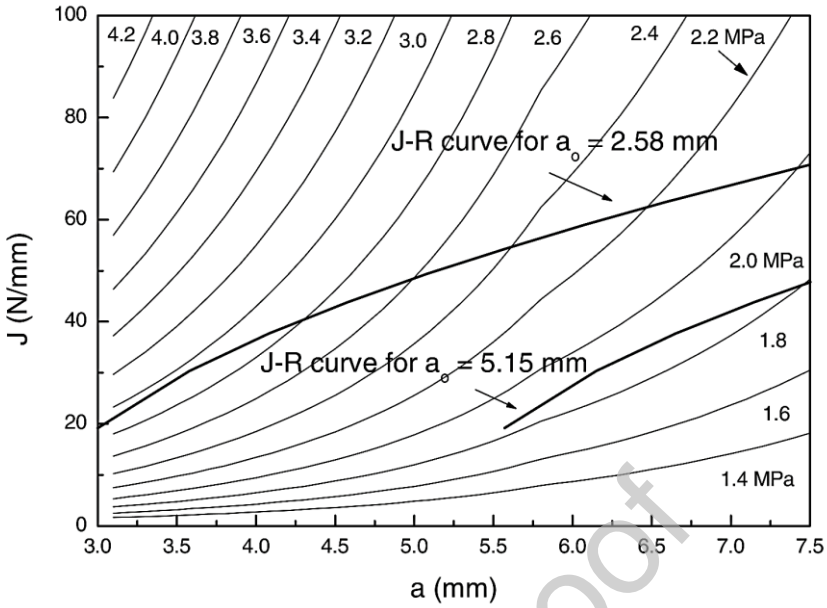

Figure 6. Driving force diagram (*J-a*) and material resistance (*J-R*) curves for an internally pressurized PE pipe with defect [89]

For the material capacity side, experimental tests are required to obtain resistance to crack opening against the driving force. These experiments have been described in ASTM D6068 and are based on compact tension or notch bending tests [86-88, 90]. For a given initial defect size, one can obtain J-crack growth resistance values (J_R) (that corresponding to a specific crack growth Δa). Thus, the relationship between J_R and Δa (i.e., *J-R* curve) can be obtained, which is typically fitted using a power-law function as shown in Equation (15) [71, 88].

$$J_R = A \cdot \Delta a^B \tag{15}$$

Where, *A* and *B* are constants and can be determined by fitting the experimental data. FE models have also been implemented to obtain *J-R* curves for the PE pipes [91, 92]. As an example, the thick solid curve in Figure 6 is a J_R curve for a PE pipe with different initial crack sizes.

In EPFM analysis, it is assumed that the crack initiation time occurs when $J > J_C$ where J_C refers to the material crack initiation toughness. According to technical committee protocol of European Structural Inspection Society (ESIS), experimental tests indicate that the initiation of crack corresponds to the value of J_R that cause 0.2 mm extension in crack front [88, 93]; thus, J_C is also denoted as $J_{0.2}$ as shown in Figure 6. As indicated in this figure, the failure happens when the gradient of *J-R* curve and *J-a* curve become equal [71].

3.3 Crack Initiation Pressure and Burst Pressure

Numerical advancements using FE models have successfully simulated crack initiation, hence reducing the needs of experimental tests. While previously experimental tests were used to determine the crack initiation toughness (J_C), the developed FE models can calculate *J* in the vicinity of the crack tip to obtain J_C for different ductile materials [83, 94, 95]. Based on the

Journal Pre-proof

numerical results, Bouaziz et al. [83] have derived the crack initiation pressure using pipe dimensions and defect size, as shown:

$$p_{cracking}(a,c,r_i,r_o,e) = \sigma_y \frac{\frac{r_o^2}{r_i^2}-1}{1+\frac{4r_o^2}{(r_o+r_i)^2}}\left(1-\sqrt{\frac{a/e}{1+\frac{0.3}{c/4r_o}}}\right) \tag{16}$$

Where, c is the crack length, e is pipe wall thickness, and r_i and r_o are inner and outer radius, respectively.

In a different study by Bouaziz et al. [96], the crack initiation pressure predicted by Equation (16) is compared with the burst pressures for PE 100 pipes with different initial defect sizes, which is shown in Figure 7 where a constant gap between crack initiation pressure and the burst pressure can be observed [83]. This offset is attributed to the crack propagation phase, which should not be ignored when the burst pressure needs to be estimated.

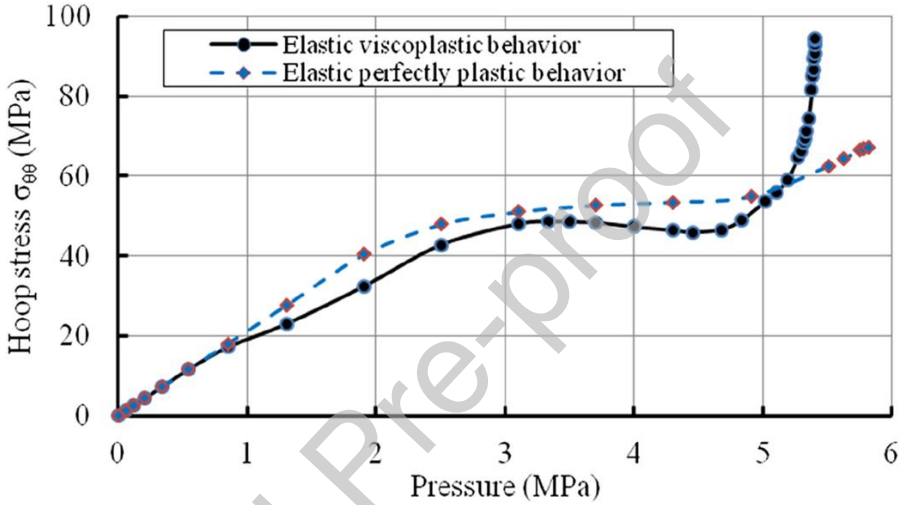

Figure 7. Comparison of burst pressures and crack initiation pressures in damaged HDPE pipes (Reproduced with permission from the journal [83])

The safety concern associated with pipelines transporting hazardous commodities such as natural gas requires special attention to the capacity of plastic pipes at fracture point. To this end, it is critical to evaluate the burst failure of PE pipes with initial defects under internal pressure. Zheng et al. [90] experimentally studied the impact of different defect shapes and sizes on the burst pressure capacity of High Density Polyethylene (HDPE) pipes; and it was found that the defects with similar depth but larger volume cause more reduction in the burst capacity, and the burst capacity does not vary with defect sizes less than 0.5 mm. In a study conducted by Lai et al. [97], the burst capacity of butt fusion welded medium density PE pipes was experimentally investigated, considering defects in welded joints. It was shown that the defects in welded joints do not change the burst capacity of the test pipes when the defects depth is less the 45% and 60% of the thickness for spherical and planar shapes. Bouaziz et al. [96] also used burst testing to determine burst pressure of PE 100 pipes with surface crack defects; and the obtained burst pressure was compared with the predicted crack initiation pressure.

To predict burst pressure capacity, Faupel [98] proposed a formula for non-defect pipes, and this formula was later modified by Majid et al. [99] to account the effect of notches on the final burst pressure of HDPE pipes, p_d, which is shown as,

Journal Pre-proof

$$p_d = \frac{2}{\sqrt{3}}\sigma_y\left(2 - \frac{\sigma_y}{\sigma_u}\right)\ln(\frac{D_0}{D_i}) \times \alpha \quad (17)$$

Where, σ_u is the ultimate strength of the material, D_0 is the outer diameter of the pipe, D_i is the inner diameter of the pipe, and α is the ratio of maximum pressure to the rupture pressure of a HDPE pipe.

Figure 8 shows the time evolution of the pressure for PE pipes with various sizes of notch in a burst test and it can be observed that the maximum pressure does not always occur at the rupture. However, to use Equation (17) to determine the rupture pressure, α needs to be determined through experimental testing on pipes with various dent sizes [99]. They concluded that the peak pressure for the undamaged pipe was obtained in the elastic phase, while for the pipes with defects, the ultimate resistance was achieved in the plastic phase.

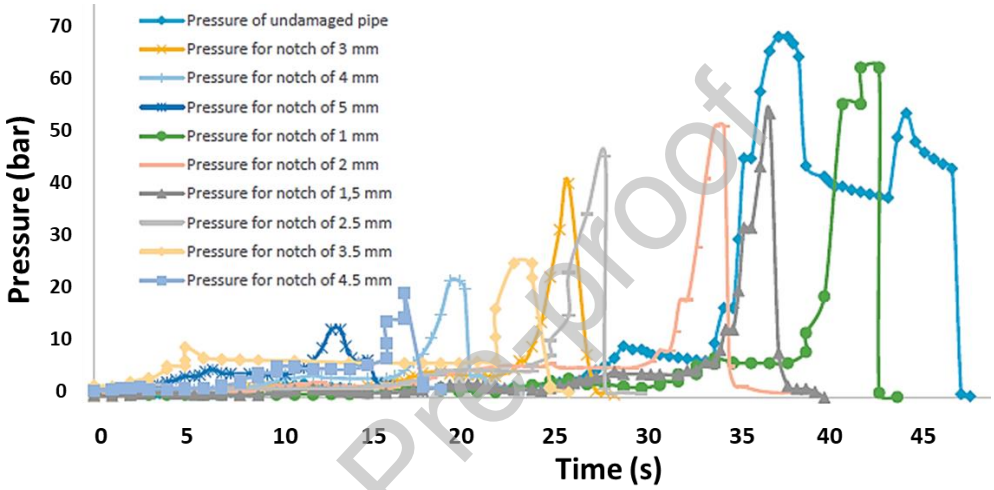

Figure 8. Pressure evolution for undamaged and notched HDPE pipes [100]

In summary, even though one could determine the burst pressure of plastic material using burst pressure tests or *J*-integral approach (that requires experiment testing), the effort towards developing a prediction model that considers initial defect geometry is still needed from a practical point of view.

3.4 Prediction Models of PE Aging

The base resin for PE is typically mixed with antioxidant stabilizer to make it chemically resistant to degradation due to oxidation process, UV radiation, and temperature variations. In summary, it is the number of free radicals in PE that autocatalyzes the polymeric chain scission. To determine the lifetime prediction, impact of diffusion of antioxidants and oxidation of PE on pipe service life need is required. Differential scanning calorimetry and differential scanning chromatography are typically used to study the consumption of antioxidants hence providing the oxidation induction time (OIT) as a function of antioxidant depletion rate (S_T) as in Equation (15) [101, 102].

$$\ln(OIT) = S_T\, t + \ln(OIT_0) \quad (15)$$

Where, t is exposure time, OIT_0 is the initial value of OIT for the unexposed pipe, and S_T is defined using similar analogies of failure rate in hydrostatic tests (16),

$$\ln(S_T) = -(E_a/\mathrm{R}'T) + \ln \mathrm{C} \quad (16)$$

Where, E_a represents the activation energy, T is absolute temperature, R′ is gas constant, and C is a temperature independent constant. Similar relations have also been reported for life prediction based on thermo-oxidative aging [103, 104].

4. Inspection Techniques for PE Pipes

Once a pipeline has been successfully tested and installed, the presence of an undetected defect or occurrence of new defect in its operating phase can cause serious consequences in case of pipe failure. The flammable nature of natural gas makes it a serious hazard if a pipeline failure occurs in a densely populated area. Therefore, it is critical to detect pipeline defects in advance through inspection to maintain the pipeline integrity, preferably in a non-destructive manner. Following are the various approaches that have been used to inspect PE pipelines.

4.1 Visual Inspection

Visual inspection is the conventional initial stage for most inspections [15, 105]. This approach requires a safety inspector to visit the site of inspection followed by performing visual analysis of the potential defects in the region of interest. This approach is usually limited to external defects given there are obvious signs of damage to be picked up by the inspector's eyes. Defects such as cracks on internal pipe walls, and internal voids/ cracks and de-bonds on fusion joints can go undetected in this approach. For buried pipeline, ground excavation may be required, which could further pose the risk of damaging the pipeline if not done properly. In addition, the outcomes of visual inspections can be subjective to inspector's expertise and experiences and cannot be considered reliable on all damage types. Considering the limitation of visual inspection on gas pipes, this approach generally needs to be supported with other inspection techniques.

4.2 Wave-Based Testing

Wave-based inspections rely on the principle of high-frequency stress waves interacting with damage present in the medium. Any potential defect in the path of wave propagation has the potential to alter the wave characteristics (e.g., amplitude, frequency, propagation speed, and phase) on the interaction [106]. However, the approach depends on various influencing factors such as inspection frequency, damage properties (geometry, orientation, and location), and structural properties (geometry and material properties). Depending on the frequency range used in the inspection, wave-based methods are usually called by the following terms: ultrasonic testing, microwave testing, tetra Hertz testing.

4.2.1 Ultrasonic testing

Conventionally ultrasonic frequency (> 20 kHz) stress waves are excited into the specimen through piezoelectric transducer-based systems and their interaction with defects is recorded either in pitch-catch or pulse-echo mode as shown schematically in Figure 9. In pitch-catch mode, wave transmission is recorded and analyzed along the propagation length of interest using a pair of transducers located on the opposite ends [107]. The arrangement for the pulse-echo method records the wave reflections from the defect interface hence providing an estimate of the damage location [108]. Both methods have their unique advantages, and the inspection choice can be limited by accessibility to the specimen surfaces, and its ability to provide

Journal Pre-proof

optimal contact to the transducers, for example, attachment of flat sensors on cylindrical pipe geometries is challenging due to its curved surface and flexible sensors might be required.

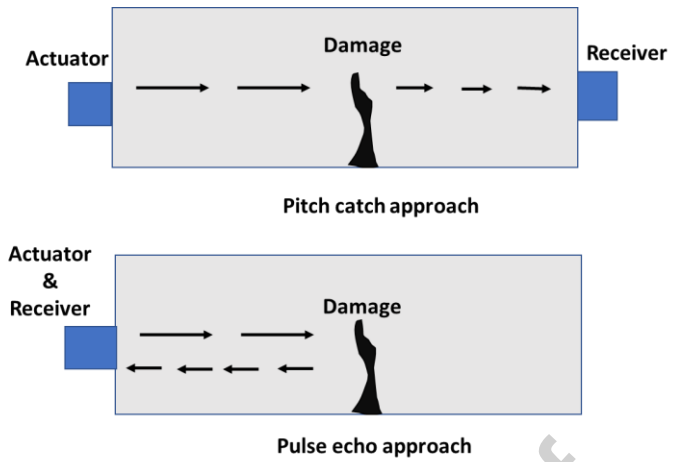

Figure 9. Schematic for different modes of wave-based inspection

Phased array ultrasonic testing (PAUT) system is commonly used to inspect defects in welded joints in PE pipes [109-112]. An array of piezoelectric transducers is used as actuators and receivers in mainly four different combinations: self-tandem, creeping wave, sector pulse-echo, and time of diffraction flight, as shown in Figure 10. The choice of transducer firing and recording pattern depends on the depth and resolution requirements for the defect inspection. The creeping wave approach provides a focus on the near-surface regions, whereas the time-of-flight diffraction provides a larger zone of inspection with limited near-surface information. PAUT has been successfully used to detect circular voids, discontinuous interfaces, and cracks [113, 114] Considering the frequency range (>1 MHz) used in the phased array methods, they are limited to the inspection of a narrow region. Such high-frequency waves cannot travel long distances due to the high attenuative properties (low elastic modulus and density) of PE. Therefore, inspection frequencies with lower attenuation are preferred for a time-efficient inspection of longer pipe lengths. The wave propagation guided by the boundaries of the pipe are then exploited to achieve long-range inspection, also known as guided wave inspection.

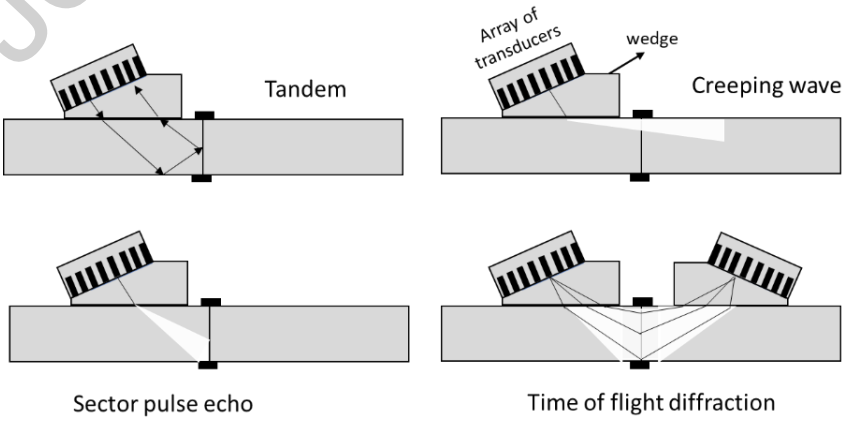

Figure 10. Different phase array techniques used for welded joints in PE pipes (Redrawn from the ref: [110])

Journal Pre-proof

The challenging aspect of guided wave propagation over a long distance in PE pipe is the complexity of wave propagation. The hollow cylindrical geometry of pipes with high wall thickness and diameter supplemented with low PE density result in the generation of multiple wave modes (torsional, flexural, longitudinal) simultaneously over a wide range of ultrasonic frequency [115]. Each mode has different acoustic properties (group velocities and attenuation), as can be seen in Figure 11, hence making the signal interpretation a challenging task. Therefore, careful consideration is required in choosing the signal shape and frequency for the inspection. Lowe et al. [116] reported the use of longitudinal modes for monitoring up to 700 mm pipe length from a single inspection point in pulse-echo configuration while using ring type transducer configuration to suppress flexural modes at the chosen inspection frequency, however no damage scenario was considered in their study. Shah et al. [117] expanded similar inspection to successfully monitor the effect of crack parameters (geometry and orientation) on the propagating longitudinal mode in a natural gas distribution PE pipe. They reported that the crack length relatively equal or greater than the frequency of the interacting wave mode is easier to detect whereas deeper crack depth is required for detecting smaller crack length. In addition, the crack orientation may restrict the ability of longitudinal mode-based inspection as axial cracks go undetected in such inspection. A relatively advanced nonlinear ultrasonic approach has been reported for detection of cracks in their incipient stage in PVC pipes by some researchers [118, 119]. The nonlinear response of micro-cracks to compressive and rarefaction phases of stress waves results in the generation of crack-induced higher order harmonics or modulated waves in the frequency spectra. However, the success of this technique on larger diameter PE pipes (resulting in dispersive wave modes) is yet to be tested. Based on the available literature, it can be argued that the application of ultrasonic testing for PE pipes is highly restricted to monitoring of welding joints despite its diversified success for damage detection in metallic pipelines.

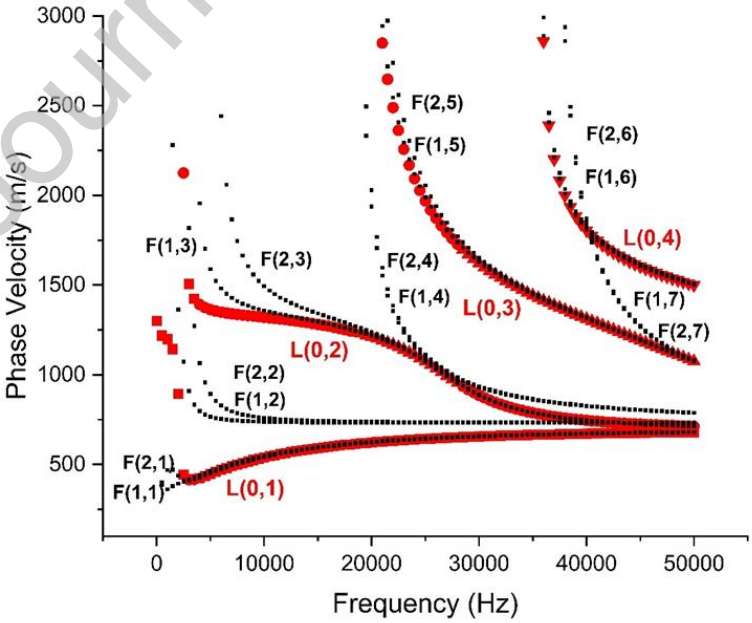

Journal Pre-proof

Figure 11: Phase velocity variation in PE (diameter: 200 mm, thickness: 20 mm) at different frequencies (F: Flexural, L: Longitudinal, m: Circumferential order, n: incremental group order number) [117]

4.2.2 Microwave Testing

Microwave inspections are relatively more favored for the inspection of dielectrics and composites given their electromagnetic nature alleviating the contact dependency as in case of ultrasonic stress waves. A typical microwave NDT system consists of surface-penetrating radar connected to a probing antenna working on the principle of reflectometry. The continuous microwave emitted by the probe interacts with the material thickness while simultaneously recording the reflectivity measurements from the area under inspection. Any discontinuity in the material in form of cracks and voids changes the relative reflectivity pattern compared to its surroundings, thereby revealing the defect location.

The investigations reported by Stakenborghs et al. [120, 121] and analogous studies [122-124] demonstrated the application of microwave NDT in identifying volumetric defects within the welded regions of PE pipes, encompassing both laboratory and field settings. The system effectively detected simulated weld discontinuities, including holes, contamination, and fine cracks within the welded regions. Shah et al. [125, 126] employed a numerical model to optimize probe frequency and antenna separations, aiming to estimate the pipe's thickness profile under various conditions. Their findings revealed the risk of overestimating defect size when probe frequency or the number of antennas is not optimized, prompting the recommendation to conduct preliminary calibration experiments on dummy cases. The exploration extends further as Wu et al. [127] and Amineh et al. [128] delve into defect imaging in concentric pipes. Both studies emphasize the need for advanced image processing methods, such as beam transformation and standardized minimum norm, to overcome resolution challenges encountered when inspecting pipe sections away from the probing antenna. Carrigan et al. [129] demonstrated the potential of a K-band (18-26.5 GHz) microwave crawler prototype in inspecting defects within PE pipes situated in three distinct environments representing overground and undersea pipelines. They reported limitations in defect detection linked to the orientation relative to the polarization of its electromagnetic field components and discussed sensitivity challenges arising from variations in the probe's distance from the pipe wall. Addressing the challenges posed by masked defect information due to pipe insulation, Buhari et al. [130] proposed a singular value decomposition method to filter out insulation-specific features from the signal. They also introduced an autofocus range-Doppler algorithm to suppress the effects of pipe curvature, ensuring compensation for the inherent noise in the raw signal. In the context of sensor development, Yu et al. [131] developed a low cost, customized microwave sensor with a coaxial waveguide section for detecting defects in PE pipes, as depicted in the Figure 12. Their work demonstrated that the presence of defects leads to a shift in the resonance frequency of the sensor and has the potential to identify flat-bottom holes.

Journal Pre-proof

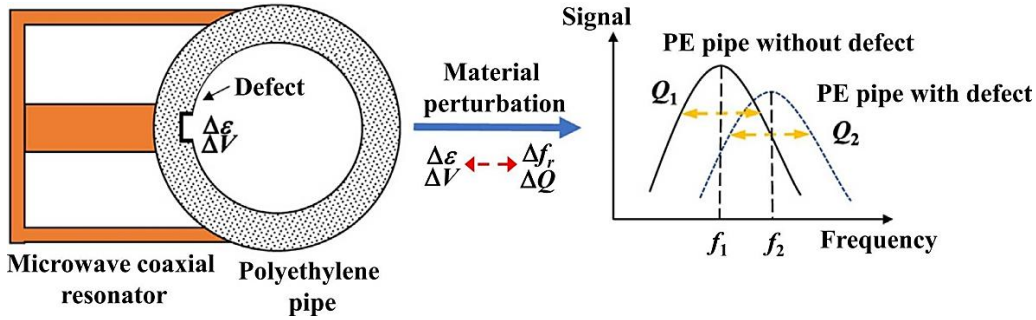

Figure 12. Concept diagram showing shift in the resonance frequency of the microwave probe in the presence of defect [131]

4.2.3. Tetrahertz Testing

The use of Tetra Hertz (THz) electromagnetic spectrum presents a distinctive advantage in the evaluation of pipeline structures. Occupying the frequency range between 0.1 to 10 THz, THz radiation offers a balanced compromise between high signal-to-noise ratio (SNR) and spatial resolution. Notably, standard polymers, including PE, exhibit transparency in the lower THz frequency range, making THz testing an attractive method for nonintrusive evaluations. Xu et al. [132] employed a THz three-dimensional imaging system based on frequency-modulated continuous-wave (FMCW) technology, showcasing its effectiveness in achieving submillimeter defect resolution for PE pipe inspection. The incorporation of a deep-learning-based THz transformer network by the researchers resulted in defect identification accuracy of up to 88%. Nei et al. [133] utilized THz time domain spectroscopy to establish a correlation between PE pipe color and THz wavelength. While successfully detecting defects in common non-black PE pipes with an error range below 10%, the researchers highlighted the necessity of higher power devices for black PE pipes, attributed to their carbon content and higher THz wave absorption. Chen et al. [134] also applied THz time domain spectroscopy for defect detection in PE gas pipes, demonstrating that variations in the maximum amplitude in the time-domain waveform indicate the presence of defects.

Weinzierl et al. [135] developed image quality indicators and concluded that THz wavelength limitations, as per Rayleigh criteria, could impact the spatial resolution of defects. In the context of pipe thickness profiling and defect imaging, it was established that phase shift and time delay data are sensitive to pipe thickness and unaffected by surface inhomogeneity, while notches of up to 2 mm size could be identified satisfactorily. Schriener et al. [136, 137] exploited the correlation between the Rayleigh resolution limit and the bandwidth of signal modulation in FMCW radar techniques to enhance defect detection in signal and multilayer plastic tubes. Their application for parallel computation on Graphic Processing Units enabled real-time calculations of layer thickness crucial for production environments. Wietzke et al. [138, 139] successfully imaged contaminated zones in the welded section of the pipe using THz imaging, illustrating that the characteristic frequency dependency of THz wave transmission can determine the size of the air gap in the weld.

Ren et al. [140] advanced beyond defect detection, demonstrating THz imaging's application in characterizing the aging degree of PE pipes using optical parameters. Their experimental findings revealed the decay of the absorption coefficient with thermal aging (Figure 13), leading to the development of an age prediction model based on a partial least square regression algorithm for various PE pipe classes. Clemens et al. [141] proposed THz tomography for inline monitoring, developing a supervised machine learning model to localize

Journal Pre-proof

defective pipe regions. The researchers emphasized the need for numerical models in such inspections due to the cost-effectiveness of expanding experimental datasets for model training. Farhat et al. [142] reported a finite element model-based study, highlighting the superiority of time domain simulations over frequency domain simulations in detecting millimeter-range discontinuities in non-metallic pipes.

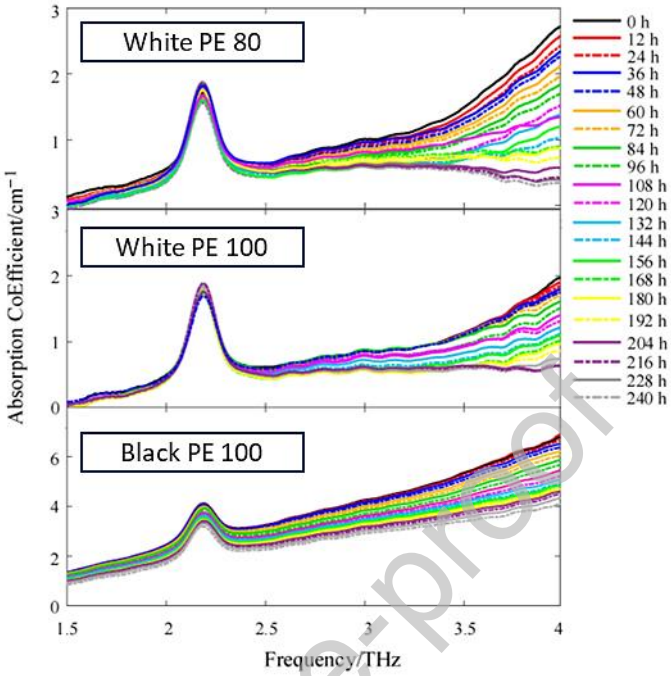

Figure 13. Absorption coefficient of three PE types with different thermal aging [140]

4.3 Infrared (IR) Thermography

Infrared thermography (IR) offers a complete reference free approach for PE pipeline inspection by detecting IR radiation emitted from the pipe's surface using an IR camera. Defects, damage, or irregularities in the pipe typically result in variations in heat dissipation, leading to distinctive thermal patterns in their vicinity. In most relevant studies, the use of active thermography has been reported, where the pipe sections under inspection are heated to generate sufficient thermal distribution.

Doaei et al. [50, 143] used IR thermography to assess the challenges of pipe ovality and misalignment of the pipe sections in the electro-fused welds. They controlled the thermal gradient of the weld by injecting a current pulse into the electrofusion coupler for a calibrated duration, ensuring no re-welding is initiated in the process. The IR images revealed the presence of defects even in the sections that passed the impact tests, typically used for determining the integrity of the weld. The main challenge in the study was to estimate the pulse duration of the current, as it was determined through a trial-and-error approach. Relevant numerical investigation reported by Azad et al. [144] mentions a finite element-based model of the coupler to determine a suitable pulsing duration across different initial temperatures, utilizing the wire inside the coupler as a heat source and using IR imaging to determine weld contaminations. The wiring pattern was approximated with the radiograph images of the coupler as shown in Figure 14a. The experimental validation established the model to be relatively more versatile than a simpler model, as reported by Shi et al. [145], which only considered heat transfer in the radial direction of the pipe. Mansouri et al. [146] reported two

Journal Pre-proof

finite difference heat transfer models to simulate thermal pulsing. The primary model approximated all heat sources in the coupler to be identical, and the latter model used geometric coefficients to distinguish the contribution of each wire ring to estimate the final solution for temperature distribution. Experimental validation established that accurate thermal distribution can be estimated by modeling thermal pulse as an unsteady state axisymmetric heat transfer problem, and geometric coefficients can be incorporated to capture the non-smooth profile of thermographic images.

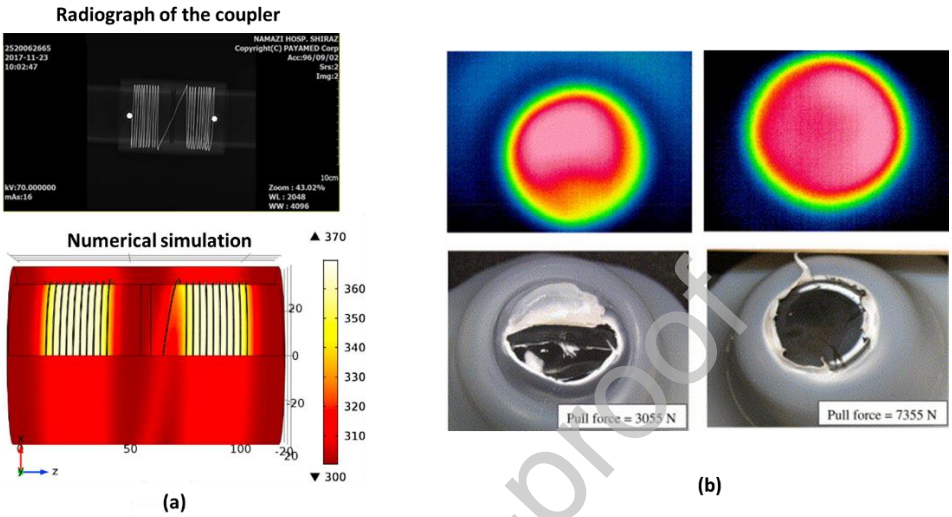

Figure 14. (a) Numerical model of the EF coupler [144] and (b) Thermograms showing adhesion uniformity and its corresponding breakage mode [23]

Kafieh et al. [24] recorded an IR video sequence of the cooling process of the freshly welded pipe to successfully investigate shortcomings in the welding process, such as unaligned pipes and incomplete scrubbing of the pipe cross-sections. To overcome the incoherency and noise inherent in the recorded images, they preprocessed the images with RGB format conversion to YUV and applied a non-linear diffusion filter. Omar et al. [23] used IR thermography to evaluate the adhesive integrity, uniformity, and bond strength of plastic welds. The thermal transmittivity across the welded section revealed the integrity of the adhesion uniformity, as demonstrated in Figure 14b. The proposed approach is a self-referencing technique [147] where the thermograph can be dissected into small local neighborhoods, and the defective behavior can be estimated with thermal contrast. Rojek et al. [22] used the thermovision technique to estimate the quality of butt-welds in the context of heat distribution across the heating tools used in the welding process. Their findings established that non-uniform temperature distribution across the heating element leads to weak welded sections; hence, periodic tests for the heat distribution of the heating element were recommended.

In another study by Zhu et al., heat transfer in the pipe was simulated by using a heating rod in the hollow section of the pipe [148]. The weak thermal profile around the weld defect was improved by using dilation and erosion transformations to adjust the grayscale values of the images, supplemented with thresholding techniques to characterize the defects. Cho et al. [149] used ultrasound-excited vibrations to create thermal hot spots in the vicinity of pipe defects. They demonstrated that outcomes of this technique are not dependent on the contact cross-section of the actuating transducer. The heat source was replaced by a tungsten lamp source in the study by Gu et al. [150], where amplitude and phase contrast in thermal images

Journal Pre-proof

highlight the pipe defects. However, the methodology required synchronization between the heat source and the IR camera.

Table 2 summarizes the pros and cons of different inspection methods discussed above.

Table 2. Summary of different studies for PE pipes

Method	Highlights	Challenges
Ultrasonic testing	• Cost effective sensors • Less labor-intensive training • Provide volumetric and long-range inspections • Can be conducted in transmission and reflection mode	• Wave attenuation in PE material • Reference of healthy pipe state is usually required • Complex guided wave mode selection • Outcomes may be subjective to surface coupling with transducers
Microwave testing	• Non-contact inspection • Better resolution than ultrasonic testing • Integration with inline robots • Customized microwave sensors can be developed	• Subjective to defect orientation • Near field inspection challenges • Overestimation of defect size if probing frequency is not optimized • Sensitive to probe placement
Tetrahertz testing	• Non-contact inspection • Balanced SNR and spatial resolution • Can be used in pulsed mode for radar applications • Used for thickness profile and defect imaging	• Higher absorption in dark colored pipes • Increased complexity in multilayers test subjects • Increased instrument cost with tailored setups
Infrared Thermography	• Complete reference free inspection • Real time visual results • Can be used to monitor welding efficiency • Inspection records are permanent for later retrieval	• Require sufficient temperature distribution on the surface • Sensitive to camera resolution • Controlling the thermal excitation of the surface is challenging • Sensitive to ambient conditions

Journal Pre-proof

5. Repair Methods for PE Pipe

The conventional pipeline repair method typically includes a pipeline excavation procedure (that involves isolating and squeezing off a large piece of pipe to stop the gas leakage), cutting out the defective portion, and then repairing the region. The repair is usually done by welding the new section to the pipe mainly through fusion. The whole repair process thus requires a large excavation site, specialized tools, and trained professionals to perform the repair, making it costly and time-inefficient especially when traffic needs to be redirected in a highly urbanized area. Therefore, many gas companies are transitioning towards keyhole isolation and adhesive-based repairs mainly for surface defects. Adhesive gels are being regularly developed and tested to repair surface defects on pipes. Following is the discussion on different repair techniques.

5.1 Fusion of PE Joints

The fusion of the new pipe section during pipeline repair follows the same process of welding as during the pipe installation. Therefore, the process of welding and the challenges remain the same. Once welded, the formed sections undergo rigorous testing to determine any leak during hydrostatic testing and the methodology can be supplemented with different NDT methods as mentioned in the above section to ensure the weld integrity.

5.1.1 Butt-fusion

Butt-fusion is the commonly used approach for joining large-diameter pipes. PE pipelines repaired with butt fusion can tolerate a long fatigue lifetime as this technique can withstand significant surge stresses [151]. Once the pipe ends to be welded are cleaned for any contamination, four specific stages in a butt-welding process are followed: (1) heating the pipe sections by pressing them against a hot plate at a predefined pressure, (2) heat soaking: as the temperature increases, the applied pressure decreases to allow time for the melted material to grow in depth, (3) hot plate removal: once the melting step is completed, the hot plate is removed, and the melted pipe ends are quickly aligned and joined together, and (4) welding and cooling: the last step involves applying a specified pressure to shape the weld into the desired appearance, leaving it to cool and solidify as summarized in Figure 15a. Despite the butt-fusion's advantages, the success of butt fusion joints is subjective to manufacturing conditions. Performing such process in a dusty and wet site location opens the pathway for weld contamination [152]. The instrumentation required is typically bulky and might not be a suitable fusion option in compact areas. In addition, misalignment of welded pipes and improper heating duration causing cold fusion are the other common issues with butt-fused joints.

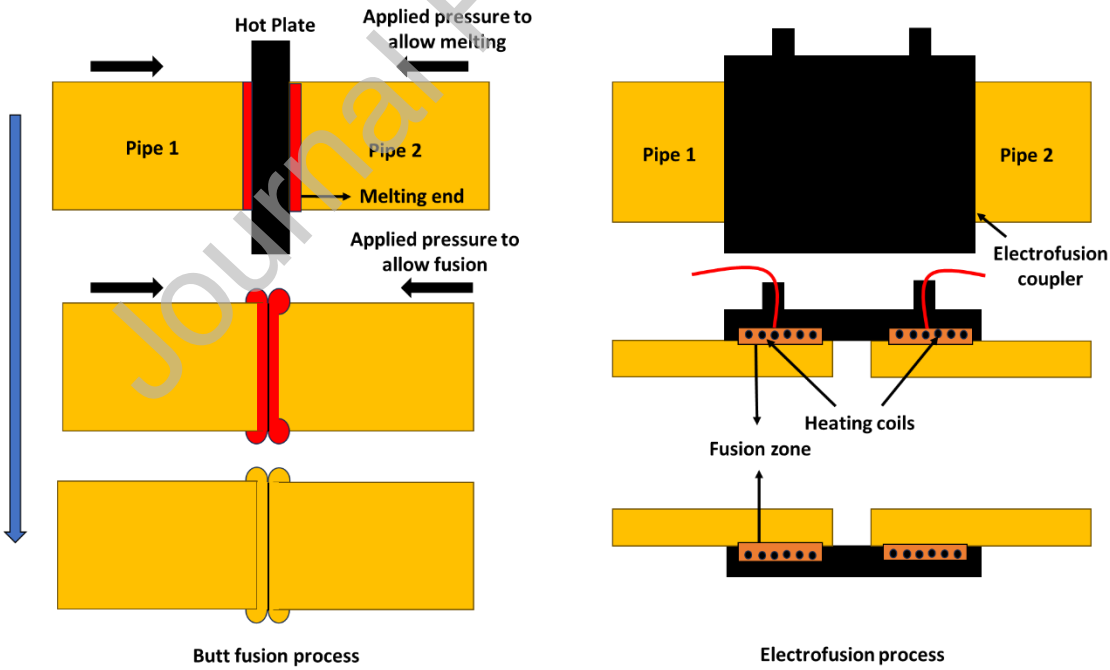

(a) (b)

Figure 15. Schematic showing (a) butt-fusion process and (b) electrofusion process

5.1.2 Electrofusion (EF)

Journal Pre-proof

Typically done on smaller diameter pipes, electrofusion (EF) welding is another welding process in which two pipe segments are welded inside a coupler [51, 153] as shown in Figure 15b. This coupler consists of molded metal wires that are used to generate heat for melting pipe material when the current is passed through them. The five main stages of EF weld are: (1) sample preparation by scrapping and cleaning the ends of pipe sections, (2) securing the pipe ends inside the coupler to achieve desired contact, (3) passing the predefined current through the coils to generate heat, (4) heat soaking to allow melting of PE for a specified duration, and (5) joint cooling to allow fusion with the coupler. EF process is known for its relatively small setup, and hence suited for applications where pulling out and cutting the defective pipe section is not feasible. Joints fused by this process are prone to leakage if not tested thoroughly [154]. Defects in EF joints can occur due to improper heat preparation to the pipe material, deficient fusion interface, over-welding, voids, and structural distortion [155]. Typically, failure of an EF welded pipe joint is caused by cracking through the fusion interface, cracking through the fitting, and cracking through the wired interface.

5.2 Adhesive Repairs of Surface Defects

Despite several advantages of PE, it is also infamous for low surface energy, rendering most adhesives ineffective for bonding PE to other materials. Tracing back to the history of patch-based PE repair, various studies by Fujimatsu et al. [156-160] demonstrated that strong adhesive bonds can be achieved by developing high-density and low-density PE gels. Polyethylene gels were prepared by dissolving PE in organic solvents at temperatures exceeding PE's melting point, followed by measuring their tensile shear strength as per relevant standards. Low-density PE gels could achieve strong adhesion when heated at 70°C compared to relatively similar strength in the case of high-density PE gels when heated at 110°C. However, a reasonable concentration of the gel needed to be determined to achieve the desired adhesive strength. It was determined that gels in solvents with higher dielectric constants offer better adhesion when heated. Takagi et al. [161] reported an alternative to PE gels where PE in its powdered form is impregnated with solvents, demonstrating strong adhesive effects when heated. The adhesive characteristics were only observed for the low-density PE powders, though. This approach also requires less solvent than that of PE gel and can be readily prepared.

Zahedi et al. [162, 163] conducted a finite element-based study to evaluate the performance of a repaired buried pipeline under different operational loads. They studied stress distribution over different defect shapes repaired with PE-based repair patches of various shapes and sizes. It was determined that irrespective of the patch shape, patch-based repairs are effective in maintaining the maximum von Mises stresses well below the allowable stress limit for PE materials as shown in Figure 16. Regad et al. [164] mentioned an economical and non-polluting hybrid composite ($90/45_2/0$) consisting of layers of perlon and glass fiber to repair defects on PE pipes. Through finite element numerical modeling, they demonstrated that the composite layer has the potential to restore the initial service pressure of the pipeline; however, long-term performance of the composite layers was not investigated. In a relatively similar study by Liamani et al. [165], it was determined that composite repair patches play a crucial role in reducing the J-integral near the crack tips by absorbing the stresses in the defective regions. The outcomes were independent of the fiber orientation in the composite. While evaluating the burst pressure of the repaired pipe sections, Hunt [166] discussed the

Journal Pre-proof

dependency of numerical results on the boundary conditions of the pipe section, as specimens with free end-fittings tend to fail at a lower pressure relative to the ones with restrained ends.

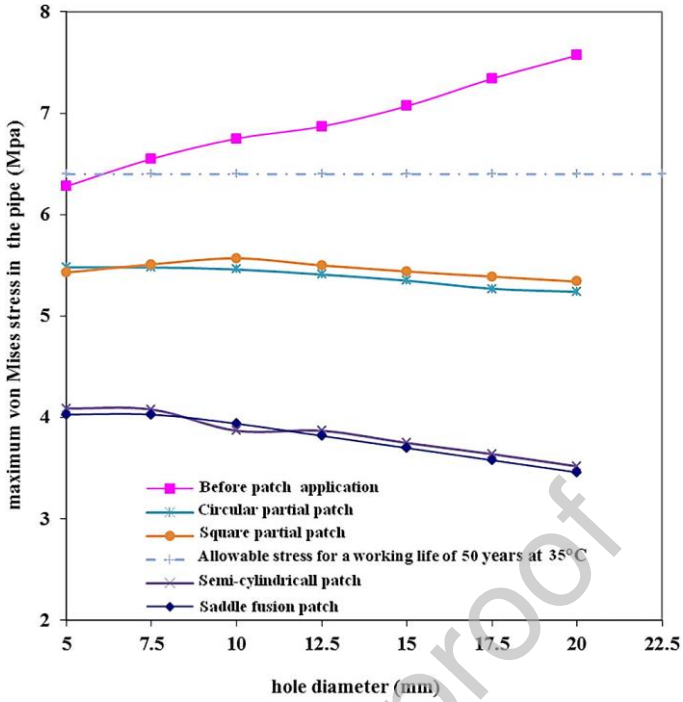

Figure 16. Maximum von Mises stress in the pipe versus defect size (diameter) for various patch shapes

Green et al. [167] developed a remote external tool to deliver thermo-chemical repair patches to the defected location in the pipeline. This tool can be used to repair PE pipelines without ground excavation, as done in butt weld repairs. They successfully conducted laboratory tests and field demonstrations to repair natural gas pipelines under line pressure, and the repair patch showed no sign of degradation under accelerated aging tests. The Gas Technology Institute reported the development of the first permanent mechanical repair sleeve for pipe repair under operating pressure [168]. In addition, the prototype also mitigated the crack growth failure mechanism, as confirmed with the analytical predictions and experimental observations. However, the performance of the prototype gave mixed results when evaluated against thermal stresses, as leakage was observed at lower temperatures.

6. Summary and future recommendations

In recent times, the overdependency on PE pipes is evident, with up to 95% of newly installed natural gas pipelines being made of PE. This is attributed to PE's lower production cost, flexibility, and corrosion resistance. Despite its numerous advantages, PE possesses a semicrystalline structure and is viscoelastic in nature, making it highly sensitive to operational loads. During its service life, PE pipes can fail under various circumstances, including crack growth due to manufacturing defects, weak weld sections, foundation settlement, and PE degradation due to thermal and chemical exposure. Considering the wide range of failure scenarios, it is crucial to develop efficient pipeline maintenance strategies. This paper provides a comprehensive review of relevant studies focused on understanding pipeline failure mechanisms, pipeline performance models, inspection methodologies, and repair methods.

Journal Pre-proof

Each section offers an overview of the conducted research and highlights key technical gaps that can be addressed in future studies. The following is a summary of these gaps:

1) Inclusion of chemical and thermal aging in life prediction models

PE as a polymer is bound to experience the effects of chemical and thermal aging, therefore, ignoring such effects in long-term performance models provides an incomplete service-life prediction, which adversely impacts risk management decision making. Further studies can be conducted to establish the potential performance prediction of an aged pipe with pre-existing defects.

2) Developing a multivariable failure prediction model

PE pipes can fail because of SCG, material degradation, and foundation settlement. It is of interest to the relevant research community to develop efficient multivariate models for predicting pipeline failures under dynamic operational conditions. These models may include the effects of pre-existing defects and transient soil bed properties sensitive to climatic and operational loads.

3) Developing robust numerical models to study wave-defect interaction

Most reported studies based on ultrasonic inspections are limited to monitoring defects in welded joints. Since SCG is a common cause of pipe failure, there is a need to explore long-range inspections of PE pipes for cracks of different orientations, geometries, and locations on pipe surfaces. Given the cost inefficiency of fabricating and testing different defect types for academic research purposes, efficient numerical models can be developed to estimate experimental outcomes. Notably, determining material damping properties is crucial for the success of such models to efficiently capture wave propagation in PE.

4) Advancement in repair methods

Incipient defects can be repaired with minimal effort in their early stages, preventing defects from progressing to dangerous levels. Given the potential of adhesive-based repairs, further research can be conducted to develop efficient adhesive patches capable of providing repairs in diverse operational conditions. It's worth noting that many reported studies were simulation-based, lacking experimental validation. Therefore, the effectiveness of repair methods needs to be evaluated under service-like conditions.

5) Regulated documentation on PE pipe inspection

Various NDT methodologies are available for pipeline inspections; however, selecting the most appropriate one can be a challenging task due to the variety of failure types in PE pipelines. Efforts can be made to develop regulated documentation for selecting the optimal inspection method specific to the type of defect. This may require collaborative initiatives between the relevant industries and academic research institutions.

Acknowledgement

The authors acknowledge the financial support provided by USDOT Pipeline and Hazardous Materials Safety Administration (PHMSA) through Competitive Academic Agreement Program (CAAP).

References

1. Schulte, U., *A vision becomes true: 50 years of pipes made from high density polyethylene.* Proceedings of Plastic Pipes XIII, 2006.

Journal Pre-proof

2. Association, A.W.W., *PE Pipe Design and Installation: M55*. Vol. 55. 2006: American Water Works Association.
3. Zodros, N., *Characterisation and degradation study of historic polyolefin gas pipes*. 2014, Manchester Metropolitan University.
4. Howard, A. ,and Rubeiz, C., *2020 Second Edition of AWWA M55 HDPE Pipe*, in *Pipelines 2020*. 2020, American Society of Civil Engineers Reston, VA. p. 277-287.
5. Yoon, D. ,and Flory, P., *Small-angle neutron scattering by semicrystalline polyethylene.* Polymer, 1977. **18**(5): p. 509-513.
6. Lustiger, A. ,and Markham, R., *Importance of tie molecules in preventing polyethylene fracture under long-term loading conditions.* Polymer, 1983. **24**(12): p. 1647-1654.
7. Reinhart, F.W., *Long-term hydrostatic strength characteristics of thermoplastics pipe.* Polymer Engineering & Science, 1966. **6**(4): p. 285-295.
8. Krishnaswamy, R.K., *Analysis of ductile and brittle failures from creep rupture testing of high-density polyethylene (HDPE) pipes.* Polymer, 2005. **46**(25): p. 11664-11672.
9. Frank, A., *Fracture mechanics based lifetime assessment and long-term failure behavior of polyethylene pressure pipes*. 2010, University of Leoben.
10. Byrne, N., De Silva, R. ,and Hilditch, T., *Linking Antioxidant Depletion with Material Properties for Polyethylene Pipes Resins.* Polymer Engineering & Science, 2020. **60**(2): p. 323-329.
11. Courtin, S., Gardin, C., Bezine, G., et al., *Advantages of the J-integral approach for calculating stress intensity factors when using the commercial finite element software ABAQUS.* Engineering Fracture Mechanics, 2005. **72**(14): p. 2174-2185.
12. Dallali, M., Azari, Z., Schmitt, C., et al., *Experimental investigations of the critical values of J-integral and crack tip opening displacement (CTOD) of high-density poly-ethylene PE100 elbow.* Engineering Failure Analysis, 2022. **131**: p. 105834.
13. Wright, D.C., *Environmental stress cracking of plastics*. 1996: iSmithers Rapra Publishing.
14. Liu, X., Zhang, H., Xia, M., et al., *Mechanical response of buried polyethylene pipelines under excavation load during pavement construction.* Engineering Failure Analysis, 2018. **90**: p. 355-370.
15. Crawford, S.L., Doctor, S.R., Cinson, A.D., et al. *Preliminary assessment of NDE methods on inspection of HDPE butt fusion piping joints for lack of fusion*. in *ASME Pressure Vessels and Piping Conference*. 2009.
16. Hekun, C., Zheng, C., Hong, C., et al. *Ultrasonic phased array inspection on PE pipe heat fusion joints and electr-fusion joints*. in *18 th World Conference in Non-Destructive Testing, Durban, South Africa*. 2012.
17. Gierulski, M.P., Tomlinson, R. ,and Troughton, M., *Electrofusion welding and reinforced thermoplastic pipes–A review.* Journal of Reinforced Plastics and Composites, 2022. **41**(3-4): p. 147-163.
18. Zheng, J., Zhang, Y., Hou, D., et al., *A review of nondestructive examination technology for polyethylene pipe in nuclear power plant.* Frontiers of Mechanical Engineering, 2018. **13**(4): p. 535-545.
19. Shafiei Alavijeh, M., Scott, R., Seviaryn, F., et al., *Using machine learning to automate ultrasound-based classification of butt-fused joints in medium-density polyethylene gas pipes.* The Journal of the Acoustical Society of America, 2021. **150**(1): p. 561-572.
20. Aleshin, N., Mogilner, L.Y., Krysko, N., et al., *Studying Applicability of TOFD Technique to Inspection of Welded Joints in Polyethylene Pipes.* Russian Journal of Nondestructive Testing, 2020. **56**(10): p. 775-783.
21. Kasban, H., Zahran, O., Arafa, H., et al., *Welding defect detection from radiography images with a cepstral approach.* Ndt & E International, 2011. **44**(2): p. 226-231.
22. Rojek, M., Stabik, J. ,and Muzia, G., *Thermography in plastics welding processes assessment.* Journal of Achievements in Materials and manufacturing Engineering, 2010. **41**(1-2): p. 40-47.
23. Omar, M., Hassan, M., Donohue, K., et al., *Infrared thermography for inspecting the adhesion integrity of plastic welded joints.* NDT & E International, 2006. **39**(1): p. 1-7.

Journal Pre-proof

24. Kafieh, R., Lotfi, T. ,and Amirfattahi, R., *Automatic detection of defects on polyethylene pipe welding using thermal infrared imaging.* Infrared Physics & Technology, 2011. **54**(4): p. 317-325.
25. Brown, N., *Slow crack growth-notches-pressurized polyethylene pipes.* Polymer Engineering & Science, 2007. **47**(11): p. 1951-1955.
26. Bergström, G., Flansbjer, M., Karlsson, L., et al., *Accpetance criteria for scratches and indentations in plastic pipes*. 2009.
27. Wang, Y. ,and Far, M.S., *Discussion of "numerical simulation of strength failure of buried polyethylene pipe under foundation settlement" by Luo et al.(2015).* Engineering Failure Analysis, 2016. **70**: p. 44-47.
28. Zhou, Z., Hiltner, A. ,and Baer, E., *Predicting long-term creep failure of bimodal polyethylene pipe from short-term fatigue tests.* Journal of materials science, 2011. **46**(1): p. 174-182.
29. Zhou, Z., Chudnovsky, A. ,and Sehanobish, K. *Evaluation of time to ductile failure in creep of PEs from short-term testing*. in *Proceedings of the 63rd annual technical conference & exhibition, ANTEC*. 2005.
30. Maupin, J. ,and Mamoun, M., *Plastic Pipe Failure, Risk, and Threat Analysis*. 2009, Gas Technology Institute.
31. Crissman, J. ,and Zapas, L., *Creep failure and fracture of polyethylene in uniaxial extension.* Polymer Engineering & Science, 1979. **19**(2): p. 99-103.
32. Crissman, J. ,and Zapas, L., *Dynamic mechanical behavior of polyethylene during creep to failure in uniaxial extension.* Journal of Applied Physics, 1977. **48**(10): p. 4049-4051.
33. Brown, N., Donofrio, J. ,and Lu, X., *The transition between ductile and slow-crack-growth failure in polyethylene.* Polymer, 1987. **28**(8): p. 1326-1330.
34. Hamouda, H.B.H., Simoes-betbeder, M., Grillon, F., et al., *Creep damage mechanisms in polyethylene gas pipes.* Polymer, 2001. **42**(12): p. 5425-5437.
35. Wang, Y., Peng, T., Lever, E., et al., *An Equivalent Creep Crack Growth Model for Probabilistic Life Prediction of Plastic Pipe Materials.* Journal of Pressure Vessel Technology, 2020. **142**(3).
36. Kalyanam, S., Krishnaswamy, P., Shim, D.-J., et al. *Assessment of slow crack growth test methodologies used to predict service life of high density polyethylene piping*. in *Pressure Vessels and Piping Conference*. 2013. American Society of Mechanical Engineers.
37. Lu, X. ,and Brown, N., *The relationship of the initiation stage to the rate of slow crack growth in linear polyethylene.* Journal of materials science, 1986. **21**: p. 2423-2429.
38. Lu, X. ,and Brown, N., *Predicting failure from the initiation stage of slow crack growth in polyethylene.* Journal of materials science, 1986. **21**: p. 4081-4088.
39. Wei, X.-F., De Vico, L., Larroche, P., et al., *Ageing properties and polymer/fuel interactions of polyamide 12 exposed to (bio) diesel at high temperature.* Npj Materials Degradation, 2019. **3**(1): p. 1-11.
40. Vogt, H., Enderle, H., Schulte, U., et al. *Thermal ageing of PE 100 pipes for accelerated lifetime prediction under service conditions*. in *International Plastic Pipe Exchange Conference*. 2009.
41. Harvey, J.A., *Chemical and physical aging of plastics*, in *Handbook of environmental degradation of materials*. 2005, Elsevier. p. 153-163.
42. Maxwell, A., Broughton, W., Dean, G., et al., *Review of accelerated ageing methods and lifetime prediction techniques for polymeric materials.* 2005.
43. Yu, W., Azhdar, B., Andersson, D., et al., *Deterioration of polyethylene pipes exposed to water containing chlorine dioxide.* Polymer degradation and stability, 2011. **96**(5): p. 790-797.
44. Yu, W., Reitberger, T., Hjertberg, T., et al., *Antioxidant consumption in squalane and polyethylene exposed to chlorinated aqueous media.* Polymer degradation and stability, 2012. **97**(11): p. 2370-2377.
45. Yu, W., Sedghi, E., Nawaz, S., et al., *Assessing the long-term performance of polyethylene stabilised with phenolic antioxidants exposed to water containing chlorine dioxide.* Polymer testing, 2013. **32**(2): p. 359-365.

Journal Pre-proof

46. Chen, G., Yang, Y., Zhou, C., et al., *Thermal-oxidative aging performance and life prediction of polyethylene pipe under cyclic and constant internal pressure.* Journal of Applied Polymer Science, 2019. **136**(28): p. 47766.
47. Pimputkar, S., *The dependence of butt fusion bond strength on joining conditions for polyethylene pipe.* Polymer Engineering & Science, 1989. **29**(19): p. 1387-1395.
48. Lu, X., Qian, R., Brown, N., et al., *The effect of pressure and contaminants on slow crack growth in a butt fusion in a polyethylene gas pipe.* Journal of applied polymer science, 1992. **46**(8): p. 1417-1427.
49. Tayefi, P., Beck, S.B. ,and Tomlinson, R.A. *Fatigue failure of polyethylene electrofusion joints subject to contamination*. in *Fracture, Fatigue, Failure, and Damage Evolution, Volume 5: Proceedings of the 2014 Annual Conference on Experimental and Applied Mechanics*. 2015. Springer.
50. Doaei, M. ,and Tavallali, M.S., *Intelligent screening of electrofusion-polyethylene joints based on a thermal NDT method.* Infrared Physics & Technology, 2018. **90**: p. 1-7.
51. Shi, J., Zheng, J., Guo, W., et al., *Defects classification and failure modes of electrofusion joint for connecting polyethylene pipes.* Journal of applied polymer science, 2012. **124**(5): p. 4070-4080.
52. Li, H., Gao, B., Dong, J., et al., *Welding effect on crack growth behavior and lifetime assessment of PE pipes.* Polymer Testing, 2016. **52**: p. 24-32.
53. Parmar, R. ,and Bowman, J., *Crack initiation and propagation paths for brittle failures in aligned and misaligned pipe butt fusion joints.* Polymer Engineering & Science, 1989. **29**(19): p. 1396-1405.
54. Guevara-Morales, A. ,and Leevers, P., *Experimental investigation of the effect of residual stresses on rapid crack propagation in polyethylene (PE100) pipes.* Polymer Engineering & Science, 2013. **53**(6): p. 1217-1222.
55. Guevara-Morales, A. ,and Leevers, P., *Experimental investigation of the effect of residual stresses and interfacial adhesion on rapid crack propagation in bilayered polypropylene/polyethylene (PP/PE 100) pipes.* Polymer Engineering & Science, 2017. **57**(4): p. 458-463.
56. Luo, X., Lu, S., Shi, J., et al., *Numerical simulation of strength failure of buried polyethylene pipe under foundation settlement.* Engineering Failure Analysis, 2015. **48**: p. 144-152.
57. Zhou, M., Wang, F., Du, Y.-J., et al., *Laboratory evaluation of buried high-density polyethylene pipes subjected to localized ground subsidence.* Acta Geotechnica, 2019. **14**(4): p. 1081-1099.
58. Zha, S. ,and Lan, H.-q., *Fracture behavior of pre-cracked polyethylene gas pipe under foundation settlement by extended finite element method.* International Journal of Pressure Vessels and Piping, 2021. **189**: p. 104270.
59. Palermo, G., Vibien, P., Oliphant, K., et al., *New test method to determine effect of recycled materials on corrugated HDPE pipe performance as projected by rate process method.* Plastics, rubber and composites, 2007. **36**(5): p. 213-218.
60. Palermo, G. *Correlating aldyl ''A''and century PE pipe rate process method projections with actual field performance*. in *Plastics Pipes XII Conference, Milan, Italy*. 2004.
61. Taherzadehboroujeni, M., Kalhor, R., Fahs, G.B., et al., *Accelerated testing method to estimate the long-term hydrostatic strength of semi-crystalline plastic pipes.* Polymer Engineering & Science, 2020. **60**(5): p. 879-888.
62. Lang, R.W., *APPLICABILITY OF LINEAR ELASTIC FRACTURE MECHANICS TO FATIGUE IN POLYMERS AND SHORT-FIBER COMPOSITES (PLASTIC ZONES, CRAZES, FRACTOGRAPHY)*. 1984: Lehigh University.
63. Hutař, P., Ševčík, M., Náhlík, L., et al., *A numerical methodology for lifetime estimation of HDPE pressure pipes.* Engineering fracture mechanics, 2011. **78**(17): p. 3049-3058.
64. Lang, R., Stern, A. ,and Doerner, G., *Applicability and limitations of current lifetime prediction models for thermoplastics pipes under internal pressure.* Die Angewandte Makromolekulare Chemie: Applied Macromolecular Chemistry and Physics, 1997. **247**(1): p. 131-145.
65. Graice, I.M., Younan, M.Y. ,and Naga, S.A.R., *Experimental investigation into the fracture toughness of polyethylene pipe material.* J. Pressure Vessel Technol., 2005. **127**(1): p. 70-75.

Journal Pre-proof

66. Frank, A., Arbeiter, F.J., Berger, I.J., et al., *Fracture mechanics lifetime prediction of polyethylene pipes.* Journal of Pipeline Systems Engineering and Practice, 2019. **10**(1): p. 04018030.
67. Pinter, G., Lang, R.W. ,and Haager, M., *A test concept for lifetime prediction of polyethylene pressure pipes.* Monatshefte für Chemie-Chemical Monthly, 2007. **138**: p. 347-355.
68. Paris, P. ,and Erdogan, F., *A critical analysis of crack propagation laws.* 1963.
69. Bouchelarm, M.A., Mazari, M. ,and Benseddiq, N., *Stress intensity factor KI and T-stress determination in HDPE material.* Journal of Failure Analysis and Prevention, 2017. **17**(5): p. 919-934.
70. Stern, A., Asanger, F. ,and Lang, R., *Creep crack growth testing of plastics—II. data acquisition, data reduction and experimental results.* Polymer testing, 1998. **17**(6): p. 423-441.
71. Burn, S., Davis, P. ,and Gould, S. *Risk analysis for pipeline assets—the use of models for failure prediction in plastics pipelines*. in *Service Life Prediction of Polymeric Materials: Global Perspectives*. 2009. Springer.
72. Al Laham, S. ,and Branch, S.I., *Stress intensity factor and limit load handbook*. Vol. 3. 1998: British Energy Generation Limited Gloucester, UK.
73. Hertzberg, R.W., Vinci, R.P. ,and Hertzberg, J.L., *Deformation and fracture mechanics of engineering materials*. 2020: John Wiley & Sons.
74. Lu, J.P., Davis, P. ,and Burn, L., *Lifetime prediction for ABS pipes subjected to combined pressure and deflection loading.* Polymer Engineering & Science, 2003. **43**(2): p. 444-462.
75. Pinter, G., Haager, M., Balika, W., et al., *Fatigue crack growth in PE-HD pipe grades.* Plastics, rubber and composites, 2005. **34**(1): p. 25-33.
76. Beech, S., Ferguson, C. ,and Clutton, E., *Mechanisms of slow crack growth in PE pipe grades.* BOOK-INSTITUTE OF MATERIALS, 2001. 7**59**: p. 401-410.
77. Nezbedová, E., Hutař, P., Zouhar, M., et al., *The applicability of the Pennsylvania Notch Test for a new generation of PE pipe grades.* Polymer Testing, 2013. **32**(1): p. 106-114.
78. Fleissner, M., *Experience with a full notch creep test in determining the stress crack performance of polyethylenes.* Polymer Engineering & Science, 1998. **38**(2): p. 330-340.
79. Schilling, M., Niebergall, U. ,and Böhning, M., *Full notch creep test (FNCT) of PE-HD–Characterization and differentiation of brittle and ductile fracture behavior during environmental stress cracking (ESC).* Polymer Testing, 2017. **64**: p. 156-166.
80. Frank, A. ,and Pinter, G., *Evaluation of the applicability of the cracked round bar test as standardized PE-pipe ranking tool.* Polymer Testing, 2014. **33**: p. 161-171.
81. Frank, A., Hutař, P. ,and Pinter, G. *Numerical assessment of PE 80 and PE 100 pipe lifetime based on Paris-Erdogan equation*. in *Macromolecular Symposia*. 2012. Wiley Online Library.
82. Lang, R., Pinter, G. ,and Balika, W., *Konzept zur Nachweisführung für Nutzungsdauer und Sicherheit von PE-Druckrohren bei beliebiger Einbausituation.* 3 R international, 2005. **44**: p. 33-41.
83. Bouaziz, M.A., Guidara, M.A., Schmitt, C., et al., *Structural integrity analysis of HDPE pipes for water supplying network.* Fatigue & Fracture of Engineering Materials & Structures, 2019. **42**(4): p. 792-804.
84. Rice, J.R., *A path independent integral and the approximate analysis of strain concentration by notches and cracks.* 1968.
85. Elmeguenni, M., Naït-Abdelaziz, M., Zaïri, F., et al., *Fracture characterization of high-density polyethylene pipe materials using the J-integral and the essential work of fracture.* International Journal of Fracture, 2013. **183**(2): p. 119-133.
86. Contino, M., Andena, L. ,and Rink, M., *Environmental stress cracking of high-density polyethylene under plane stress conditions.* Engineering Fracture Mechanics, 2021. **241**: p. 107422.
87. Lai, H.S., Tun, N.N., Yoon, K.B., et al., *Effects of defects on failure of butt fusion welded polyethylene pipe.* International Journal of Pressure Vessels and Piping, 2016. **139**: p. 117-122.
88. Han, L.-h., Deng, Y.-c. ,and Liu, C.-d., *The determination of JIC for polyethylene pipe using non-standard arc-shaped specimen.* International journal of pressure vessels and piping, 1999. **76**(9): p. 647-651.

Journal Pre-proof

89. Kumar, V., German, M. ,and Shih, C.F., *Engineering approach for elastic-plastic fracture analysis*. 1981, General Electric Co.
90. Zheng, X., Wang, J. ,and Chen, H., *Burst pressures of high-density polyethylene pipes considering the notch effect: testing and prediction.* Journal of Testing and Evaluation, 2020. **48**(6).
91. Broberg, K.B., *Cracks and fracture*. 1999: Elsevier.
92. Benhamena, A., Aminallah, L., Bouiadjra, B.B., et al., *J integral solution for semi-elliptical surface crack in high density poly-ethylene pipe under bending.* Materials & Design, 2011. **32**(5): p. 2561-2569.
93. Machado, R., Gonzalez, M. ,and Gonzalez, J. *Experimental study of crack growth in HDPE PE100 pipes*. in *Pressure Vessels and Piping Conference*. 2013. American Society of Mechanical Engineers.
94. Roos, E. ,and Eisele, U., *Determination of material characteristic value in elastic-plastic fracture mechanics by means of J-integral crack resistance curves.* Journal of testing and evaluation, 1988. **16**(1): p. 1-11.
95. Huang, D.D., *The application of fracture mechanics to materials selection.* Polymer Engineering & Science, 1996. **36**(18): p. 2270-2274.
96. Bouaziz, M., Guidara, M., Dallali, M., et al. *Collapse analysis of longitudinally cracked HDPE pipes*. in *Design and Modeling of Mechanical Systems—III: Proceedings of the 7th Conference on Design and Modeling of Mechanical Systems, CMSM'2017, March 27–29, Hammamet, Tunisia 7*. 2018. Springer.
97. Lai, H.S., Tun, N.N., Kil, S.H., et al., *Effect of defects on the burst failure of butt fusion welded polyethylene pipes.* Journal of Mechanical Science and Technology, 2016. **30**: p. 1973-1981.
98. Faupel, J. ,and Furbeck, A., *Influence of residual stress on behavior of thick-wall closed-end cylinders.* Transactions of the American Society of Mechanical Engineers, 1953. **75**(3): p. 345-354.
99. MAJID, F., *Damage Assessment of HDPE Thermoplastics Pipes.* Journal of Advanced Research in Physics, 2017. **6**(2).
100. Majid, F., Ouardi, A., Barakat, M., et al., *Mechanical behavior prediction of PPR and HDPE polymers through newly developed nonlinear damage-reliability models.* Procedia Structural Integrity, 2017. **3**: p. 387-394.
101. Allen, N.S., Hoang, E., Liauw, C.M., et al., *Influence of processing aids on the thermal and photostabilisation of HDPE with antioxidant blends.* Polymer degradation and stability, 2001. **72**(2): p. 367-376.
102. Phease, T., Billingham, N. ,and Bigger, S., *The effect of carbon black on the oxidative induction time of medium-density polyethylene.* Polymer, 2000. **41**(26): p. 9123-9130.
103. Wang, Y., Lan, H.-q. ,and Zhang, H. *A Residual Lifetime Prediction Method of Aging Polyethylene Gas Pipes in Service*. in *Pressure Vessels and Piping Conference*. 2019. American Society of Mechanical Engineers.
104. Celina, M.C., *Review of polymer oxidation and its relationship with materials performance and lifetime prediction.* Polymer Degradation and Stability, 2013. **98**(12): p. 2419-2429.
105. See, J.E., Drury, C.G., Speed, A., et al. *The role of visual inspection in the 21st century*. in *Proceedings of the Human Factors and Ergonomics Society Annual Meeting*. 2017. SAGE Publications Sage CA: Los Angeles, CA.
106. Olisa, S.C., Khan, M.A. ,and Starr, A., *Review of current guided wave ultrasonic testing (GWUT) limitations and future directions.* Sensors, 2021. **21**(3): p. 811.
107. Jolly, M.R., Prabhakar, A., Sturzu, B., et al., *Review of non-destructive testing (NDT) techniques and their applicability to thick walled composites.* Procedia CIRP, 2015. **38**: p. 129-136.
108. Frederick, C., Porter, A. ,and Zimmerman, D., *High-density polyethylene piping butt-fusion joint examination using ultrasonic phased array.* Journal of pressure vessel technology, 2010. **132**(5).
109. Hagglund, F., Robson, M., Troughton, M.J., et al. *A novel phased array ultrasonic testing (PAUT) system for on-site inspection of welded joints in plastic pipes*. in *Proceedings of the*

Journal Pre-proof

11th European Conference on Non-Destructive Testing (ECNDT), Prague, Czech Republic. 2014.

110. Hagglund, F., Spicer, M.A. ,and Troughton, M.J. *Phased array ultrasonic testing of welded joints in plastic (PE) pipes*. in *6th Middle East Nondestructive Testing Conference*. 2012.
111. Hagglund, F., Spicer, M.A. ,and Troughton, M.J. *Detection capabilities of a phased array ultrasonic inspection system for plastic pipe butt fusion joints*. in *51st Annual Conference of British Institute of Non-Destructive Testing*. 2012.
112. Qin, Y., Shi, J., Zheng, J., et al., *An improved phased array ultrasonic testing technique for thick-wall polyethylene pipe used in nuclear power plant.* Journal of Pressure Vessel Technology, 2019. **141**(4).
113. Zheng, J., Zhang, Y., Hou, D., et al., *A review of nondestructive examination technology for polyethylene pipe in nuclear power plant.* Frontiers of Mechanical Engineering, 2018. **13**: p. 535-545.
114. Zheng, J., Qin, Y., Shi, J., et al. *Classification of Defects in Fusion Joints of Polyethylene Pipes*. in *Pressure Vessels and Piping Conference*. 2010.
115. Rose, J.L., *Ultrasonic waves in solid media*. 2000, Acoustical Society of America.
116. Lowe, P.S., Lais, H., Paruchuri, V., et al., *Application of ultrasonic guided waves for inspection of high density polyethylene pipe systems.* Sensors, 2020. **20**(11): p. 3184.
117. Shah, J., El-Hawwat, S. ,and Wang, H., *Guided Wave Ultrasonic Testing for Crack Detection in Polyethylene Pipes: Laboratory Experiments and Numerical Modeling.* Sensors, 2023. **23**(11): p. 5131.
118. Demčenko, A., Akkerman, R., Nagy, P., et al., *Non-collinear wave mixing for non-linear ultrasonic detection of physical ageing in PVC.* Ndt & E International, 2012. **49**: p. 34-39.
119. Wang, Q., Zhou, H., Xie, J., et al., *Nonlinear ultrasonic evaluation of high-density polyethylene natural gas pipe thermal butt fusion joint aging behavior.* International Journal of Pressure Vessels and Piping, 2021. **189**: p. 104272.
120. Stakenborghs, R. ,and Little, J. *Microwave based NDE inspection of HDPE pipe welds*. in *International Conference on Nuclear Engineering*. 2009.
121. Stakenborghs, R.J. *Innovative technique for inspection of polyethylene piping base material and welds and non-metallic pipe repair*. in *ASME Pressure Vessels and Piping Conference*. 2006.
122. Zhu, X.W., Pan, J.P. ,and Tan, L.J. *Microwave scan inspection of HDPE piping thermal fusion welds for lack of fusion defect*. in *Applied Mechanics and Materials*. 2013. Trans Tech Publ.
123. Murphy, K. ,and Lowe, D. *Evaluation of a novel microwave based NDT inspection method for polyethylene joints*. in *Pressure Vessels and Piping Conference*. 2011.
124. Pan, J.-p., Hu, J., Zhu, X.-w., et al. *Identifying lack of fusion defects in high-density polyethylene piping welds*. in *2016 IEEE Far East NDT New Technology & Application Forum (FENDT)*. 2016. IEEE.
125. Shah, M.B., Gao, Y., Ravan, M., et al., *Quantitative defect size evaluation in fluid-carrying nonmetallic pipes.* IEEE Transactions on Microwave Theory and Techniques, 2022. **70**(8): p. 4071-4081.
126. Shah, M.B., Gao, Y., Ravan, M., et al. *Thickness profile estimation of fluid-carrying non-metallic pipes*. in *2022 IEEE/MTT-S International Microwave Symposium-IMS 2022*. 2022. IEEE.
127. Wu, H., Ravan, M., Sharma, R., et al. *Non-Destructive Testing of Non-Metallic Concentric Pipes Using Microwave Measurements*. in *2020 IEEE/MTT-S International Microwave Symposium (IMS)*. 2020.
128. Amineh, R.K., Ravan, M. ,and Sharma, R., *Nondestructive Testing of Nonmetallic Pipes Using Wideband Microwave Measurements.* IEEE Transactions on Microwave Theory and Techniques, 2020. **68**(5): p. 1763-1772.
129. Carrigan, T.D., Forrest, B.E., Andem, H.N., et al., *Nondestructive testing of nonmetallic pipelines using microwave reflectometry on an in-line inspection robot.* IEEE Transactions on Instrumentation and Measurement, 2018. **68**(2): p. 586-594.

Journal Pre-proof

130. Buhari, M.D., Tian, G.Y. ,and Tiwari, R., *Microwave-Based SAR Technique for Pipeline Inspection Using Autofocus Range-Doppler Algorithm.* IEEE Sensors Journal, 2019. **19**(5): p. 1777-1787.
131. Yu, H., Jin, Q., Meng, Z., et al., *Detection of defects in polyethylene pipes using open microwave coaxial line resonator sensor.* Sensors and Actuators A: Physical, 2023. **358**: p. 114427.
132. Xu, J., Zhang, Z., Yang, P., et al., *Nondestructive testing and 3D imaging of PE pipes using terahertz frequency-modulated continuous wave.* Applied Optics, 2022. **61**(34): p. 10230-10239.
133. Nie, H., Hao, F., Wang, L., et al., *Application of Terahertz Nondestructive Testing Technology in the Detection of Polyethylene Pipe Defects.* ACS omega, 2023. **8**(30): p. 27323-27332.
134. Chen, Q., Wang, Q., Yu III, Y., et al. *Inspection of polyethylene gas pipe defect based on terahertz time domain spectroscopy*. in *Tenth International Conference on Information Optics and Photonics*. 2018. SPIE.
135. WEINZIERL, J., SCHMIDT, L., RUTZ, F., et al., *Imaging Capability of Terahertz and Millimeter-Wave Instrumentations for NDT of Polymer Materials.*
136. Schreiner, N., Baccouche, B., Sauer-Greff, W., et al. *High-resolution FMCW millimeter-wave and terahertz thickness measurements*. in *2017 47th European Microwave Conference (EuMC)*. 2017. IEEE.
137. Schreiner, N.S., Sauer-Greff, W., Urbansky, R., et al., *Multilayer thickness measurements below the Rayleigh limit using FMCW millimeter and terahertz waves.* Sensors, 2019. **19**(18): p. 3910.
138. Wietzke, S., Krumbholz, N., Jördens, C., et al. *Inspection of plastic weld joints with terahertz imaging*. in *Optical Measurement Systems for Industrial Inspection V*. 2007. SPIE.
139. Wietzke, S., Jördens, C., Krumbholz, N., et al., *Terahertz imaging: a new non-destructive technique for the quality control of plastic weld joints.* Journal of the European Optical Society-Rapid Publications, 2007. **2**.
140. Ren, J., Xu, J., Zhang, D., et al., *Terahertz Spectroscopy Characterization and Prediction of the Aging Degree of Polyethylene Pipes Based on PLS.* Materials, 2023. **16**(10): p. 3652.
141. Meiser, C., Schuster, T. ,and Wald, A. *A classification algorithm for anomaly detection in terahertz tomography*. in *International Conference on Large-Scale Scientific Computing*. 2021. Springer.
142. Farhat, M., Amer, A., Cunningham, V., et al., *Numerical modeling for terahertz testing of non-metallic pipes.* AIP Advances, 2020. **10**(9).
143. Doaei, M., Tavallali, M.S. ,and Nejati, H., *Fault classification in electrofusion polyethylene joints by combined machine learning, thermal pulsing and IR thermography methods–A comparative study.* Infrared Physics & Technology, 2019. **96**: p. 262-266.
144. Azad, M.J. ,and Tavallali, M.S., *A novel computational supplement to an IR-thermography based non-destructive test of electrofusion polyethylene joints.* Infrared Physics & Technology, 2019. **96**: p. 30-38.
145. Shi, J., Zheng, J., Guo, W., et al., *A model for predicting temperature of electrofusion joints for polyethylene pipes.* 2009.
146. Mansouri, S. ,and Tavallali, M.S., *Heat transfer approximate modeling, parameter estimation and thermography of thermal pulsing in electrofusion joints of gas pipelines.* Infrared physics & technology, 2019. **98**: p. 354-363.
147. Omar, M., Hassan, M., Saito, K., et al., *IR self-referencing thermography for detection of in-depth defects.* Infrared physics & technology, 2005. **46**(4): p. 283-289.
148. Zhu, Z., Zhong, S., Qiu, X., et al., *Nondestructive Defect Evaluation of Polyethylene Pipes.* WSEAS Transactions on Applied and Theoretical Mechanics, 2016. **11**: p. 107-113.
149. Cho, J.-W., Seo, Y.-C., Jung, S.-H., et al., *Defect detection within a pipe using ultrasound excited thermography.* Nuclear Engineering and Technology, 2007. **39**(5): p. 637-646.
150. GU, J., LEE, H. ,and LEE, C., *NDE of the Internal Defect of PVC Pipe using Infrared Lock-in Thermography.*
151. Lai, H.S., Tun, N.N., Kil, S.H., et al., *Effect of defects on the burst failure of butt fusion welded polyethylene pipes.* Journal of Mechanical Science and Technology, 2016. **30**(5): p. 1973-1981.

Journal Pre-proof

152. Zhao, J.Q., Daigle, L. ,and Beaulieu, D., *Effect of joint contamination on the quality of butt-fused high-density polyethylene (HDPE) pipe joints.* Canadian Journal of Civil Engineering, 2002. **29**(5): p. 787-798.
153. Bowman, J., *A review of the electrofusion joining process for polyethylene pipe systems.* Polymer Engineering & Science, 1997. **37**(4): p. 674-691.
154. Fujikake, M., Fukumura, M. ,and Kitao, K., *Analysis of the electrofusion joining process in polyethylene gas piping systems.* Computers & structures, 1997. **64**(5-6): p. 939-948.
155. Ge, Z., Yao, R., Shi, J., et al. *A Comprehensive Review on Failure Analysis of Electrofusion Joint For Plastic Pipes*. in *Pressure Vessels and Piping Conference*. 2021. American Society of Mechanical Engineers.
156. Fujimatsu, H., Ogasawara, S. ,and Kuroiwa, S., *Swollen polyethylene films as adhesives to bond polyethylene moldings.* Journal of adhesion science and technology, 1990. **4**(1): p. 35-40.
157. Fujimatsu, H., Satoh, N., Yamamoto, S., et al., *Effect of solvents on adhesion between polyethylene moldings and molten polyethylenes.* Composite Interfaces, 1994. **2**(2): p. 117-125.
158. Fujimatsu, H., Ogasawara, S., Satoh, N., et al., *Adhesive effect of low-density polyethylene gels on polyethylene moldings.* Colloid and Polymer Science, 1990. **268**: p. 143-147.
159. Fujimatsu, H., Ogasawara, S., Satoh, N., et al., *Adhesive effect of high density polyethylene gels on polyethylene moldings.* Colloid and Polymer Science, 1989. **267**: p. 500-505.
160. Fujimatsu, H., Ogasawara, S. ,and Kuroiwa, S., *Adhesion of molded polyethylene using polyethylene gels by microwave heating.* Colloid and Polymer Science, 1990. **268**: p. 28-30.
161. Takagi, K., Fujimatsu, H., Karaki, H., et al., *Effect of polyethylene powder impregnated with solvents on adhesion between two polyethylene moldings.* Composite Interfaces, 1995. **3**(3): p. 243-252.
162. Khademi-Zahedi, R. ,and Shishesaz, M., *Application of a finite element method to stress distribution in buried patch repaired polyethylene gas pipes.* Underground Space, 2019. **4**(1): p. 48-58.
163. Khademi Zahedi, R., Alimouri, P., Khademi Zahedi, H., et al., *Investigating peak stresses in fitting and repair patches of buried polyethylene gas pipes.* Frontiers of Structural and Civil Engineering, 2020. **14**: p. 147-168.
164. Regad, A., Benzerga, D., Berrekia, H., et al., *Repair and rehabilitation of corroded HDPE100 pipe using a new hybrid composite.* Frattura ed Integrità Strutturale, 2021. **15**(56): p. 115-122.
165. Liamani, S. ,and Abderahmane, S., *Modeling the Repair of a Crack in an HDPE Pipe.* Periodica Polytechnica Mechanical Engineering, 2021. **65**(2): p. 134-140.
166. Hunt, J., *The testing and repair of polyethylene natural gas distribution pipe.* 2004.
167. Green, K.H., Rochefort, W.E., Wannenmacher, N., et al., *Development of a remote external repair tool for damaged or defective polyethylene pipe*. 2006, Timberwolf Corp.
168. Patadia, H., *Development of Permanent Mechanical Repair Sleeve for Plastic Pipe*. 2005, Gas Technology Institute.

Journal Pre-proof

Graphical Abstract

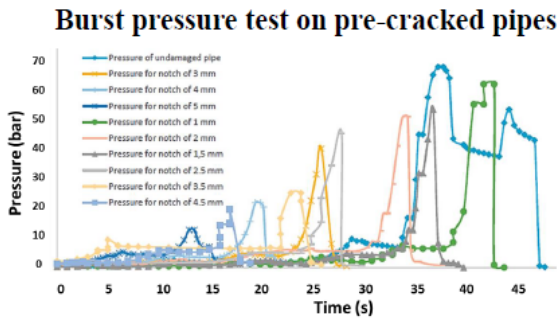

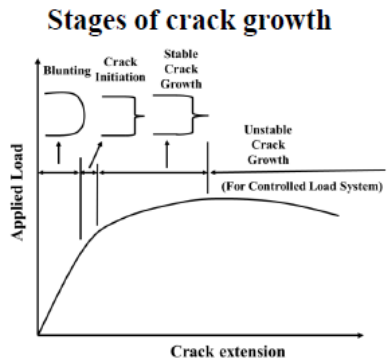

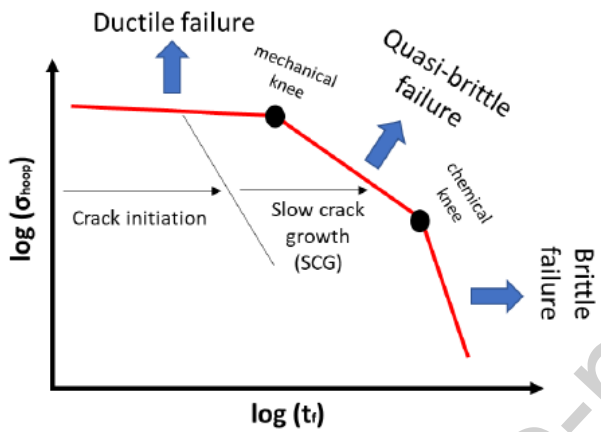

Failure curve for a PE pipe

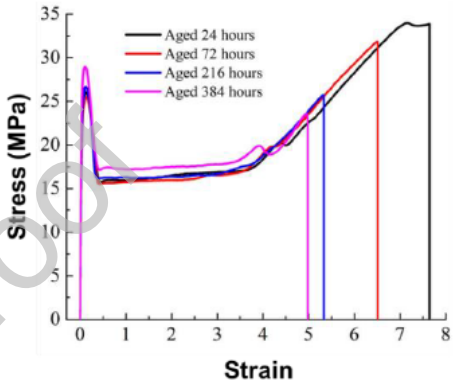

Aging effects on PE

Conflicts of Interest

The authors declare that they have no conflict of interest.

Journal Pre-proof